Table 1. Association between clinicopathological characteristics of patients and *FHL1* promoter methylation

Characteristics	FLH1 methylation		P
	Positive (N = 21)	Negative (N = 59)	
Tumor invasion			
≤T2	13	33	0.80
>T2	8	26	
Lymph node metastasis			
Positive	15	50	0.20
Negative	6	9	
Histological type			
Intestinal	8	27	0.61
Diffuse	13	32	
CIMP			
Positive	17	13	2.9×10^{-6}
Negative	4	46	
EBV infection			
Positive	4	1	0.02
Negative	17	58	
hMLH1 *methylation*			
Positive	4	5	0.23
Negative	17	54	

Abbreviations: CIMP, CGI methylator phenotype; EBV, Epstein–Barr virus.

FHL1 methylation to the formation of an epigenetic field defect, *FHL1* methylation levels were quantified in gastric mucosae of male healthy volunteers (with and without *H. pylori* infection; 16 each) and non-cancerous mucosae of male gastric cancer patients (with and without *H. pylori* infection; 26 each) (Figure 6a). Among the healthy volunteers, *FHL1* methylation was elevated only in *H. pylori*-positive individuals (10 of 16, 62.5%; $P = 0.01$, *t*-test). As potent methylation induction by *H. pylori* can mask a difference in *H. pylori*-positive individuals,[8] *FHL1* methylation levels were compared between healthy volunteers and gastric cancer patients among the *H. pylori*-negative individuals. *FHL1* methylation level was shown to be elevated only in gastric cancer patients (5 of 26, 19.2%; $P = 0.09$, *t*-test). In the case of the colon, *FHL1* methylation was elevated in colonic mucosae of only 2 of 50 colon cancer patients (4%) (Supplementary Figure 5).

FHL1 methylation levels in female specimens

FHL1 methylation levels were analyzed in female specimens, including gastric mucosae of healthy volunteers (18 with *H. pylori* infection and 10 without), those of gastric cancer patients (7 with *H. pylori* infection and 11 without) and one specimen of peripheral leukocytes (Figure 6b). As in male specimens, among the healthy volunteers, *FHL1* methylation levels were significantly elevated in *H. pylori*-positive individuals ($P = 0.01$, *t*-test). Among the *H. pylori*-negative individuals, they tended to be higher in cancer patients than those in healthy volunteers ($P = 0.06$, *t*-test). *FHL1* methylation levels in *H. pylori*-negative female specimens were expected to be 50% because *FHL1* is located on chromosome X, but its actual distribution was between 20 and 40%. Bisulfite sequencing of the *FHL1* promoter region showed that female specimens contained DNA molecules with sparse methylation of CpG sites (Figure 6c), which was in contrast with the dense methylation in cancer specimens (Figure 3b). It was considered that the inactive chromosome X had sparse methylation of the *FHL1* promoter region not detected by qMSP.

DISCUSSION

The *FHL1* gene on chromosome X was shown to be a tumor-suppressor gene in gastrointestinal cancers by the presence of its methylation-silencing, its inhibitory effects on migration, invasion and growth, and the presence of a loss-of-function mutation. Notably, a loss-of-function mutation was identified for the first time in any type of cancers. This added *FHL1* as a new member of 'risky' tumor-suppressor genes on chromosome X, and the first tumor-suppressor gene on chromosome X that can be inactivated by methylation-silencing. *FHL1* methylation was associated with *H. pylori* infection and strongly accumulated in gastric mucosae of gastric cancer patients. Together with the fact that *FHL1* is a tumor-suppressor gene, the accumulation of *FHL1* methylation was considered to contribute to the formation of a field for cancerization as a driver.

Downregulation of *FHL1* in surgical specimens has been reported in breast, renal, prostate,[23] gastric,[25] liver,[21] and lung cancers.[22] The downregulation was associated with short patient survival and deep invasion in gastric cancers,[25] and with poor differentiation in lung cancers.[22] As a mechanism for the downregulation, methylation silencing was described in bladder cancers.[24] Functionally, *FHL1* has been reported to suppress growth of lung, liver and breast cancer cells and transformed fibroblasts,[21,22,26,30] and migration and invasion of bladder cancer cells and transformed fibroblasts.[24,26] The data obtained here were in line with previous reports, and demonstrated that *FHL1* inhibits migration and invasion in gastrointestinal cancer cells.[22]

Mechanistically, FHL1 is characterized by the presence of four and a half highly conserved LIM domains, which are involved in a wide range of protein–protein interactions, including actin cytoskeleton, cellular signaling proteins and transcriptional machinery.[31] In hepatocellular carcinomas, FHL1 was shown to interact with Smad2 and activate TGF-β pathway independently of TGF-β.[21] In breast cancers, FHL1 was shown to interact with estrogen receptor-α and estrogen receptor-β, and repress estrogen-responsive gene transcription.[30] Proteins that interact with FHL1 in gastric and colonic epithelial cells have not been clarified yet. However, inactivation of the TGF-β pathway is known to be involved in these cancers,[32] and is a strong candidate mechanism of how *FHL1* inactivation is involved in these gastrointestinal cancers.

FHL1 methylation was present not only in cancer tissues, but also in non-cancerous gastric mucosae of gastric cancer patients (5 of 26) and in non-cancerous colonic mucosae of colon cancer patients (2 of 50). This showed, for the first time in any types of cancers, that *FHL1* methylation silencing is involved in the formation of the epigenetic field defect as a driver. So far, only a limited number of driver genes, including *CDKN2A*, *CDH1* and *LOX*, are known to be involved in the formation of an epigenetic field defect.[18] For those genes on autosomes, it is difficult to estimate what fraction of cells has biallelic methylation. In contrast, in the case of *FHL1*, its methylation level linearly correlates with the fraction of cells with its inactivation, and, even if its methylation level is low, the presence of its methylation is expected to bring a significant impact. *H. pylori* infection is known to induce aberrant methylation that consists of temporary and permanent components,[8,33] and the high methylation levels in individuals with current *H. pylori* infection were in accordance with this previous finding.

In females, approximately half of the DNA molecules were methylated densely or sparsely, in gastric mucosae and peripheral leukocytes of healthy volunteers without *H. pylori* infection by bisulfite sequencing. As no methylated DNA molecules were detected in a male specimen, both the densely and sparsely methylated DNA molecules in female specimens were considered to be derived from the inactive X allele.[34] However, we were not able to demonstrate it because a polymorphism that can

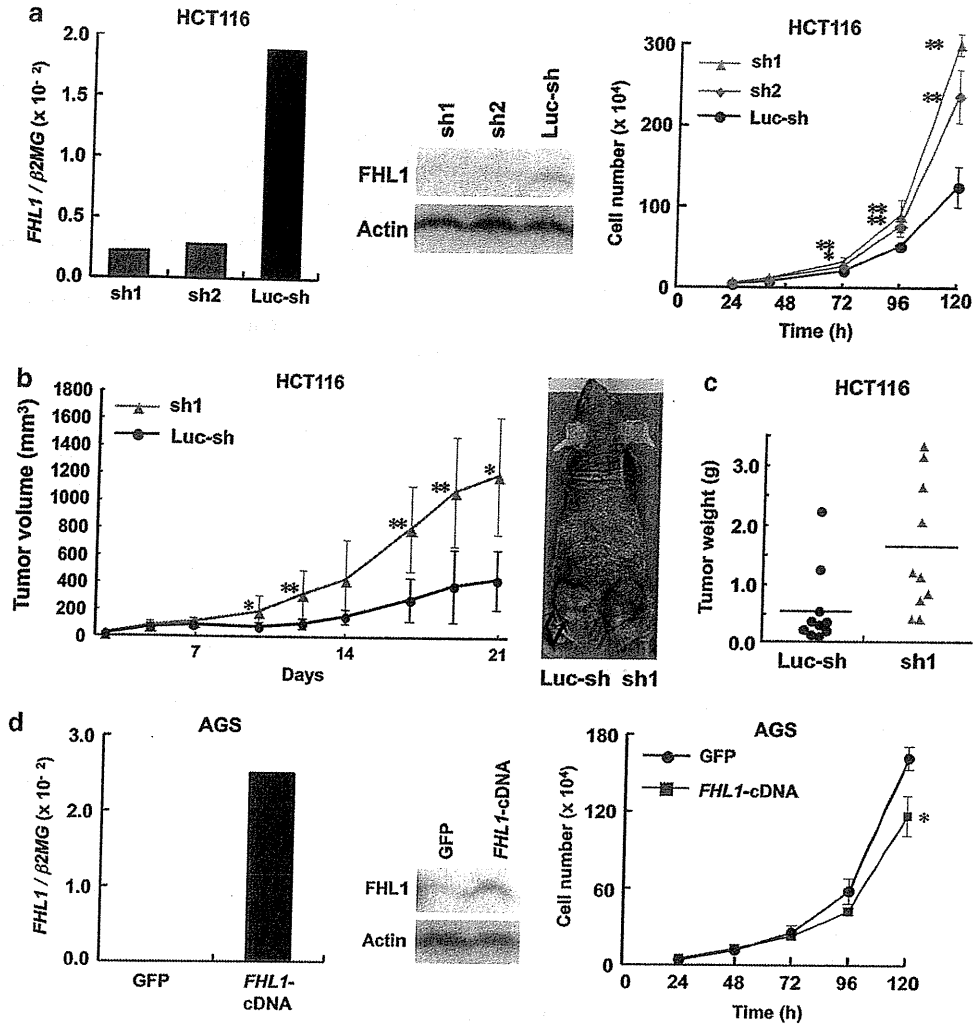

Figure 4. Growth-suppressive activity of *FHL1 in vitro* and *in vivo*. (**a**) *FHL1* knockdown and the resultant increased growth of HCT116 cells. Decreased expression of *FHL1* by its knockdown was confirmed by qRT–PCR (left) and western blot (middle). Growth rates of cells with *FHL1* knockdown were shown to be increased (*$P<0.01$, **$P<0.001$) (right). Data are shown as the mean of three independents ± s.d. (**b**) Increased *in vivo* growth of HCT116 cells with *FHL1* knockdown. Cells with *FHL1* knockdown (sh1) showed a 2.7-fold larger tumor volume compared with the control cells (Luc-sh) (*$P<0.01$, **$P<0.001$). Data are shown as the mean ± s.d. Arrows, tumors produced. (**c**) Increased tumor weight of cells with *FHL1* knockdown (sh1). Mean tumor weight of cells with knockdown (sh1) ($n=10$) was 2.8-fold heavier than that of controls (Luc-sh) ($n=10$). (**d**) Exogenous *FHL1* expression and the resultant decreased growth of AGS cells. Increased levels of *FHL1* expression were confirmed by qRT–PCR (left) and western blot (middle). Growth rates of cells with exogenous *FHL1* were shown to be significantly decreased (*$P<0.01$) (right).

distinguish the allelic origin of mRNA was not present. As qMSP detects only molecules that have dense methylation at primer sites, it was considered that it detected only densely methylated molecules, and methylation levels between 20 and 40% were observed in females.

In conclusion, we showed that *FHL1* on chromosome X is a methylation-silenced tumor-suppressor gene in gastrointestinal cancers, and its methylation in non-cancerous gastric mucosae contributes to the formation of an epigenetic field for cancerization.

MATERIALS AND METHODS

Cell lines and treatment with 5-aza-dC

Sixty-eight cancer cell lines (6 gastric, 7 colon, 12 lung, 12 skin, 7 pancreas, 4 esophageal, 4 prostate, 6 breast and 10 ovary cancer cell lines) and two normal colonic epithelial cells (CRL1790 and CRL1831) were obtained from the American Type Culture Collection (Manassas, VA, USA), Japanese Collection of Research Bioresources (Tokyo, Japan), RIKEN Cell Bank (Tsukuba, Japan) and Tohoku University Cell Resource Center for Biomedical Research (Sendai, Japan)(Supplementary Table 2). HSC39, HSC44 and HSC57 were gifted by Dr K Yanagihara; TMK1 was gifted by Dr W Yasui at Hiroshima University; and GC2 was established by MT For 5-aza-dC treatment. AGS and KATOIII cells were seeded on day 0; media containing freshly prepared 0.3 μM 5-aza-dC were added on days 1 and 3, and cells were harvested on day 5.[35]

Tissue specimens and analysis of *H. pylori* infection status

Cancer specimens were obtained from 80 male gastric cancer patients (average age = 60.4, range = 29–88) and 144 male colon cancer patients (average age = 70, range = 39–98) who underwent gastric and colon resection, respectively, with informed consent. All cancers were histologically diagnosed, and histological types of gastric cancers were classified according to the Lauren classification system (35 intestinal and 45 diffuse type).[36] EBV positivity was determined by *in situ* hybridization targeting *EBER1* using formalin-fixed and paraffin-embedded specimens.[37] The proportion of EBV-positive specimens (5 of 80, 6.3%) was close to EBV prevalence in a previous report (11 of 172, 6.4%).[38]

Normal appearing gastric mucosae were obtained by endoscopic biopsy of the antral region from 60 healthy volunteers (32 male and 28 female; average age = 52, range = 25–91) and 70 gastric cancer patients

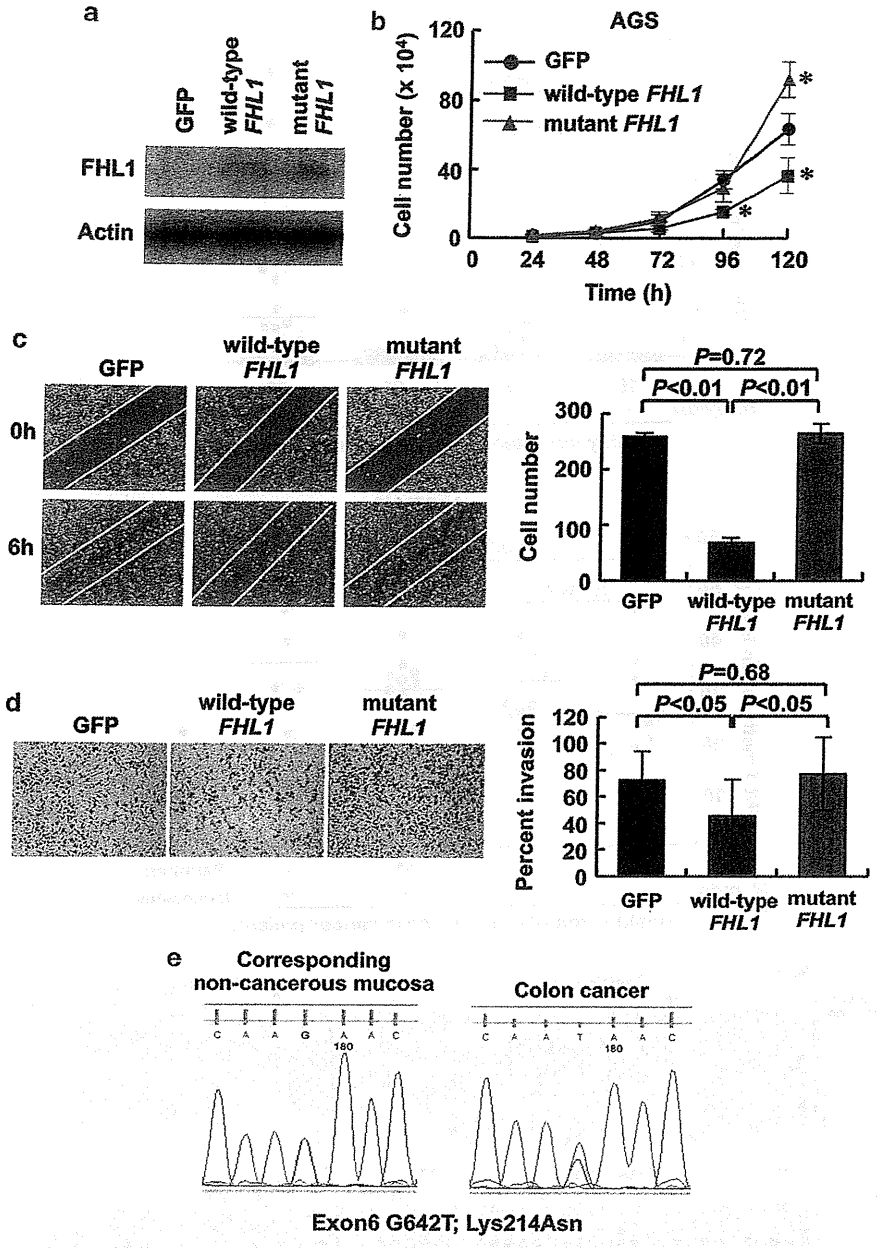

Figure 5. Inhibitory effects of *FHL1* on migration and invasion, and the lack of such functions in *FHL1* with the G642T mutation in AGS. (**a**) Expression levels of exogenous wild-type and mutant *FHL1* detected by western blot. (**b**) The growth-suppressive effect of the wild-type *FHL1*, and the lack of the effect in mutant *FHL1*. Whereas wild-type *FHL1* suppressed cell growth, mutant *FHL1* did not (*$P<0.01$). (**c**) Migration inhibition by wild-type *FHL1*, and the lack of the effect in the mutant *FHL1*. Whereas wild-type *FHL1* inhibited cell migration to 26.6% of the control cells, mutant *FHL1* did not. Photographs were taken at 0 and 6 h after scratching (left), and the number of cells that migrated into the scratched area was counted (mean ± s.d.; right). (**d**) Invasion inhibition by wild-type *FHL1*, and the lack of the effect in the mutant *FHL1*. Whereas wild-type *FHL1* inhibited cell invasion, mutant *FHL1* did not. Representative fields with invading cells on Matrigel-precoated membrane (left). Percent invasion is shown as the mean ± s.d. (right). (**e**) Sequence analysis of colon cancer specimens and corresponding non-cancerous colonic mucosae showed a somatic mutation (G642T; Lys214Asn) in exon 6 of *FHL1*.

(52 male and 18 female; average age = 65, range = 38–85). *H. pylori* infection status was analyzed by a serum anti-*H. pylori* IgG antibody test (SRL, Tokyo, Japan), rapid urease test (Otsuka, Tokushima, Japan) or culture test (Eiken, Tokyo, Japan). Gastric epithelial cells for qRT-PCR analysis were isolated by the gland isolation technique.[39] Normal-appearing colonic mucosae were obtained from a mucosal area distant from colon cancers of surgically resected specimens. Leukocytes were collected from one male (age = 47) and one female (age = 32) volunteer. Specimens were kept frozen at −80 °C until DNA/RNA extraction. All the analyses using human-derived specimens were approved by the Institutional Review Boards.

Data processing of expression microarray analysis

Expression microarray analysis data in our previous report[19] were used. Signal intensities were scaled so that average signal intensity of all the 18 602 genes would become 500.

Sodium bisulfite modification, MSP, qMSP and bisulfite sequencing

Bisulfite modification was performed using 1 μg of *Eco*RI-digested genomic DNA as previously described.[40] MSP was performed with

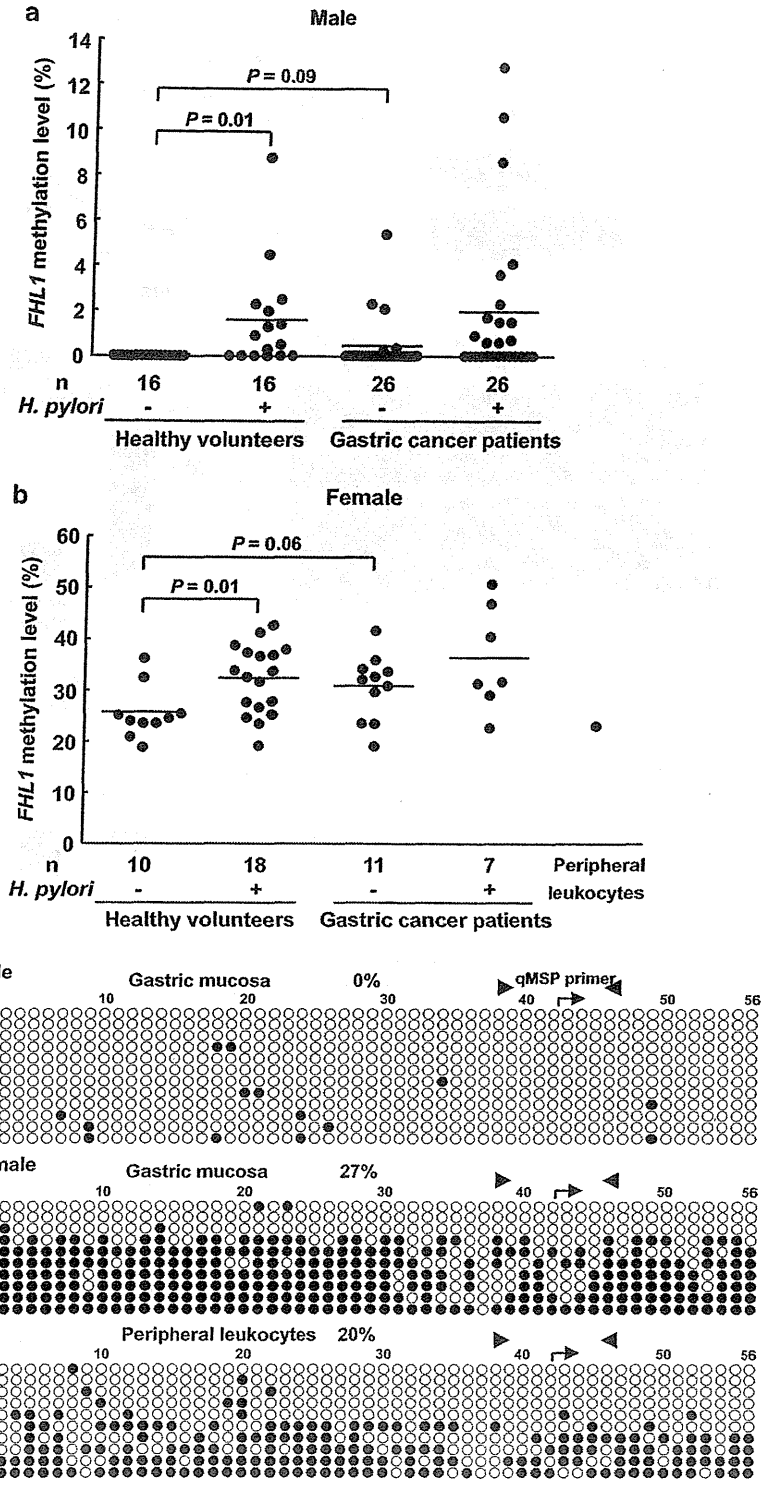

Figure 6. *FHL1* methylation levels in male and female gastric mucosae. (a) Methylation levels in male gastric mucosae of healthy volunteers and non-cancerous mucosae of gastric cancer patients. A horizontal line represents the mean methylation level for each group. Among healthy volunteers, *FHL1* methylation was present only in *H. pylori*-positive individuals ($P = 0.01$). Among individuals without *H. pylori* infection, *FHL1* methylation was present only in gastric cancer patients. (b) Methylation levels in female gastric mucosae and peripheral leukocytes. *FHL1* methylation levels distributed between 20 and 40%. Methylation levels were higher in *H. pylori*-positive healthy volunteers and gastric cancer patients also in female. (c) Bisulfite sequencing of male gastric mucosae, female gastric mucosae and female peripheral leukocytes. Female specimens contained both densely methylated and sparsely methylated DNA molecules, and it was considered that the inactive chromosome X can be densely and sparsely methylated. Closed circle, methylated CpG site; open circle, unmethylated CpG site; arrowheads, primers for qMSP; and arrow, transcription start site.

primer sets specific to methylated and unmethylated sequences (Supplementary Table 3). As controls, fully methylated and unmethylated DNA were prepared by methylating genomic DNA with *SssI* methylase (New England Biolabs, Beverly, MA, USA) and by amplifying genomic DNA with the GenomiPhi amplification system (GE Healthcare, Buckinghamshire, UK), respectively.

Quantitative real-time MSP was performed by real-time PCR using SYBR Green I (BioWhittaker Molecular Applications, Rockland, ME, USA) and an iCycler Thermal Cycler (Bio-Rad Laboratories, Hercules, CA, USA). Although a primer set for MSP was also used for qMSP, a specific annealing temperature in the presence of SYBR Green I was determined (Supplementary Table 3). The number of molecules in a specimen was determined by comparing its amplification with those of standard DNA that contained known numbers of molecules (10^1–10^6 molecules). Based on the numbers of methylated (M) and unmethylated (U) molecules, a methylation level was calculated as the fraction of M molecules in the total number of DNA molecules (no. of M molecules + no. of U molecules). Standard DNA was prepared by cloning PCR products of methylated and unmethylated sequences into a vector (pGEM-T Easy, Promega, Madison, WI, USA). The CIMP status in a gastric cancer was determined as described previously.[27]

Bisulfite sequencing was conducted with primers common to methylated and unmethylated DNA sequences (Supplementary Table 4). The PCR product was cloned into pGEM-T Easy, and 10–12 clones were cycle-sequenced for each specimen.

qRT–PCR

cDNA was synthesized from 1 μg of total RNA using a Superscript III (Invitrogen, Carlsbad, CA, USA). qRT–PCR was performed by real-time PCR using SYBR Green I and an iCycler Thermal Cycler. Standard DNA was prepared by serial dilution of PCR products quantified by the QIAxcel system (QIAGEN, Valencia, CA, USA) after purification using Zymo-Spin I Columns (Zymo Research, Orange, CA, USA).[41] The measured number of cDNA molecules was normalized to that of b2-microglobulin (*b2MG*). The primers and PCR conditions are shown in Supplementary Table 5.

Knockdown and cDNA introduction assays

For a knockdown assay, two pairs and one pair of oligonucleotides were designed against *FHL1* and *Luciferase* (control), respectively (Supplementary Table 6). After annealing of sense and antisense oligonucleotides, the fragment was cloned into a pGreenPuro lentiviral vector (System Biosciences, Mountain View, CA, USA). For cDNA cloning, the entire coding region of human *FHL1* was amplified by RT–PCR (Supplementary Table 7), and cloned into a pCDH-CMV-MCS-EF1-Puro lentiviral vector (System Biosciences). As a control, *copGFP* was cloned into the vector in the same manner. The mutant cDNA was synthesized using the site-directed mutagenesis technique.[42] Using complementary primers carrying mutated sequence (mutation site forward and reverse primers; Supplementary Table 7) and primers for each end of the entire coding region (entire region reverse and forward primers), RT–PCR was performed to generate two DNA fragments that had overlapping ends. These two PCR products were combined by a subsequent PCR with primers for each end of the entire coding region to obtain the mutant cDNA. The mutant cDNA was cloned into a pCDH-CMV-MCS-EF1-Puro lentiviral vector.

The viral vectors and packaging vectors (pPACKH1 HIV Lentivector Packaging Kit, System Biosciences) were cotransfected into 293TN packaging cells, and culture media-containing pseudoviral particles were retrieved. Infection of cancer cell lines with pseudoviral particles was performed according to the manufacturer's protocol (System Biosciences), and stably expressing cells were selected by puromycin without cloning.

Cell growth, migration, invasion and apoptosis analysis

Cell growth was analyzed by seeding cells in triplicate in a six-well plate (3×10^4 cells, AGS; 1×10^5 cells, HSC39) and in a 12-well plate (5×10^3 cells, HCT116). Their numbers were counted at 24, 48, 72, 96 and 120 h. Three independent cultures were performed for one experiment.

Cell migration was analyzed by a wound-healing assay.[13] Cells were seeded in triplicate in a 6-cm dish coated with type I collagen (1×10^6 cells, AGS; 4×10^6 cells, MKN28), and cultured in RPMI-1640 medium containing 1% fetal calf serum to form a monolayer. The cell monolayer was scraped in a straight line with a pipette tip. After incubation for 6 and 12 h, the migrating cells were observed under bright-field microscopy. Three independent cultures were performed for one experiment.

Cell invasion was analyzed by a Matrigel invasion assay, using a Boyden chamber with the Matrigel-precoated membrane or Matrigel-free membrane in the top chamber (BD Biosciences, Bedford, MA, USA). Cells were seeded in top chambers in serum-free RPMI1640 (5×10^4 cells, AGS; 1×10^5 cells, MKN28), and the bottom chambers were filled with RPMI1640 containing 10% fetal calf serum. After incubation for 24 and 48 h (AGS and MKN28, respectively), the area of cells invading through the top chambers was measured by ImageJ software (version 1.38, National Institutes of Health, Bethesda, MD, USA). Percent invasion was calculated as the area of cells invading through the Matrigel-precoated membrane relative to those through Matrigel-free membrane. Three independent cultures were performed for one experiment and the experiment was repeated three times.

The apoptosis of the cells was analyzed by terminal deoxynucleotidyl transferase dUTP nick end labeling assay, using an *in situ* cell death detection kit, TMRred (Roche, Basel, Switzerland).

Tumor formation assay in nude mice

Cells (8×10^6 cells, HCT116) were inoculated subcutaneously on both flanks of 7-week-old male athymic nude mice (BALB/cAJc1-nu/nu; CLEA, Tokyo, Japan). Tumor sizes were measured with calipers every 3 days and the volume was calculated as (length × width^2) × 0.5, and tumor weights were measured at their killing on day 22. All the animal experiments were approved by the Animal Experiment Ethical Committee at the National Cancer Center.

Mutation analysis

All seven exons of *FHL1* were amplified using 100 ng of genomic DNA with primers located in introns, except for one primer on exon 7 (Supplementary Table 8). The PCR products were directly cycle-sequenced with a BigDye Terminator kit (PE Biosystems, Foster City, CA, USA) and an ABI PRISM 310 automated DNA sequencer (PE Biosystems).

Statistical analysis

Differences in mean methylation levels, expression levels, cell numbers and tumor sizes were analyzed by the Welch *t*-test. Association between *FHL1* methylation and clinicopathological factors was analyzed by the χ^2 test. All the analyses were performed using SPSS (SPSS, Inc., Chicago, IL, USA), and the results were considered significant when a P value < 0.05 was obtained by two-sided tests.

CONFLICT OF INTEREST

The authors declare no conflict of interest.

ACKNOWLEDGEMENTS

We thank Dr Yanagihara and Dr Yasui for their kind gift of cell lines. This study was supported by a Grant-in-Aid for the Third-term Comprehensive Cancer Control Strategy from the Ministry of Health, Labour and Welfare, Japan, and by the National Cancer Center Research and Development Fund. TA is a recipient of the Research Resident Fellowship from the Foundation for Promotion of Cancer Research.

REFERENCES

1 Knudson AG. Two genetic hits (more or less) to cancer. *Nat Rev Cancer* 2001; 1: 157–162.
2 Ushijima T. Detection and interpretation of altered methylation patterns in cancer cells. *Nat Rev Cancer* 2005; 5: 223–231.
3 Jones PA, Baylin SB. The epigenomics of cancer. *Cell* 2007; 128: 683–692.
4 Rivera MN, Kim WJ, Wells J, Driscoll DR, Brannigan BW, Han M *et al*. An X chromosome gene, WTX, is commonly inactivated in Wilms tumor. *Science* 2007; 315: 642–645.
5 Zuo T, Wang L, Morrison C, Chang X, Zhang H, Li W *et al*. FOXP3 is an X-linked breast cancer suppressor gene and an important repressor of the HER-2/ErbB2 oncogene. *Cell* 2007; 129: 1275–1286.
6 Wang L, Liu R, Li W, Chen C, Katoh H, Chen GY *et al*. Somatic single hits inactivate the X-linked tumor suppressor FOXP3 in the prostate. *Cancer Cell* 2009; 16: 336–346.
7 Van Vlierberghe P, Palomero T, Khiabanian H, Van Der Meulen J, Castillo M, Van Roy N *et al*. PHF6 mutations in T-cell acute lymphoblastic leukemia. *Nat Genet* 2010; 42: 338–342.

8 Maekita T, Nakazawa K, Mihara M, Nakajima T, Yanaoka K, Iguchi M *et al.* High levels of aberrant DNA methylation in Helicobacter pylori-infected gastric mucosae and its possible association with gastric cancer risk. *Clin Cancer Res* 2006; **12**: 989–995.
9 Ando T, Yoshida T, Enomoto S, Asada K, Tatematsu M, Ichinose M *et al.* DNA methylation of microRNA genes in gastric mucosae of gastric cancer patients: its possible involvement in the formation of epigenetic field defect. *Int J Cancer* 2009; **124**: 2367–2374.
10 Shen L, Kondo Y, Rosner GL, Xiao L, Hernandez NS, Vilaythong J *et al.* MGMT promoter methylation and field defect in sporadic colorectal cancer. *J Natl Cancer Inst* 2005; **97**: 1330–1338.
11 Kondo Y, Kanai Y, Sakamoto M, Mizokami M, Ueda R, Hirohashi S. Genetic instability and aberrant DNA methylation in chronic hepatitis and cirrhosis—a comprehensive study of loss of heterozygosity and microsatellite instability at 39 loci and DNA hypermethylation on 8 CpG islands in microdissected specimens from patients with hepatocellular carcinoma. *Hepatology* 2000; **32**: 970–979.
12 Ishii T, Murakami J, Notohara K, Cullings HM, Sasamoto H, Kambara T *et al.* Oesophageal squamous cell carcinoma may develop within a background of accumulating DNA methylation in normal and dysplastic mucosa. *Gut* 2007; **56**: 13–19.
13 Oka D, Yamashita S, Tomioka T, Nakanishi Y, Kato H, Kaminishi M *et al.* The presence of aberrant DNA methylation in noncancerous esophageal mucosae in association with smoking history: a target for risk diagnosis and prevention of esophageal cancers. *Cancer* 2009; **115**: 3412–3426.
14 Lee YC, Wang HP, Wang CP, Ko JY, Lee JM, Chiu HM *et al.* Revisit of field cancerization in squamous cell carcinoma of upper aerodigestive tract: better risk assessment with epigenetic markers. *Cancer Prev Res* 2011; **4**: 1982–1992.
15 Yan PS, Venkataramu C, Ibrahim A, Liu JC, Shen RZ, Diaz NM *et al.* Mapping geographic zones of cancer risk with epigenetic biomarkers in normal breast tissue. *Clin Cancer Res* 2006; **12**: 6626–6636.
16 Arai E, Kanai Y, Ushijima S, Fujimoto H, Mukai K, Hirohashi S. Regional DNA hypermethylation and DNA methyltransferase (DNMT) 1 protein overexpression in both renal tumors and corresponding nontumorous renal tissues. *Int J Cancer* 2006; **119**: 288–296.
17 Nakajima T, Maekita T, Oda I, Gotoda T, Yamamoto S, Umemura S *et al.* Higher methylation levels in gastric mucosae significantly correlate with higher risk of gastric cancers. *Cancer Epidemiol Biomarkers Prev* 2006; **15**: 2317–2321.
18 Ushijima T. Epigenetic field for cancerization. *J Biochem Mol Biol* 2007; **40**: 142–150.
19 Yamashita S, Tsujino Y, Moriguchi K, Tatematsu M, Ushijima T. Chemical genomic screening for methylation-silenced genes in gastric cancer cell lines using 5-aza-2′-deoxycytidine treatment and oligonucleotide microarray. *Cancer Sci* 2006; **97**: 64–71.
20 Ushijima T, Watanabe N, Shimizu K, Miyamoto K, Sugimura T, Kaneda A. Decreased fidelity in replicating CpG methylation patterns in cancer cells. *Cancer Res* 2005; **65**: 11–17.
21 Ding L, Wang Z, Yan J, Yang X, Liu A, Qiu W *et al.* Human four-and-a-half LIM family members suppress tumor cell growth through a TGF-beta-like signaling pathway. *J Clin Invest* 2009; **119**: 349–361.
22 Niu C, Liang C, Guo J, Cheng L, Zhang H, Qin X *et al.* Downregulation and growth inhibitory role of FHL1 in lung cancer. *Int J Cancer* 2012; **130**: 2549–2556.
23 Li X, Jia Z, Shen Y, Ichikawa H, Jarvik J, Nagele RG *et al.* Coordinate suppression of Sdpr and Fhl1 expression in tumors of the breast, kidney, and prostate. *Cancer Sci* 2008; **99**: 1326–1333.
24 Matsumoto M, Kawakami K, Enokida H, Toki K, Matsuda R, Chiyomaru T *et al.* CpG hypermethylation of human four-and-a-half LIM domains 1 contributes to migration and invasion activity of human bladder cancer. *Int J Mol Med* 2010; **26**: 241–247.
25 Sakashita K, Mimori K, Tanaka F, Kamohara Y, Inoue H, Sawada T *et al.* Clinical significance of loss of Fhl1 expression in human gastric cancer. *Ann Surg Oncol* 2008; **15**: 2293–2300.
26 Shen Y, Jia Z, Nagele RG, Ichikawa H, Goldberg GS. SRC uses Cas to suppress Fhl1 in order to promote nonanchored growth and migration of tumor cells. *Cancer Res* 2006; **66**: 1543–1552.
27 Enomoto S, Maekita T, Tsukamoto T, Nakajima T, Nakazawa K, Tatematsu M *et al.* Lack of association between CpG island methylator phenotype in human gastric cancers and methylation in their background non-cancerous gastric mucosae. *Cancer Sci* 2007; **98**: 1853–1861.
28 Ota N, Kawakami K, Okuda T, Takehara A, Hiranuma C, Oyama K *et al.* Prognostic significance of p16(INK4a) hypermethylation in non-small cell lung cancer is evident by quantitative DNA methylation analysis. *Anticancer Res* 2006; **26**: 3729–3732.
29 Matsusaka K, Kaneda A, Nagae G, Ushiku T, Kikuchi Y, Hino R *et al.* Classification of Epstein-Barr virus-positive gastric cancers by definition of DNA methylation epigenotypes. *Cancer Res* 2011; **71**: 7187–7197.
30 Ding L, Niu C, Zheng Y, Xiong Z, Liu Y, Lin J *et al.* FHL1 interacts with oestrogen receptors and regulates breast cancer cell growth. *J Cell Mol Med* 2011;**15**: 72–85.
31 Shathasivam T, Kislinger T, Gramolini AO. Genes proteins and complexes: the multifaceted nature of FHL family proteins in diverse tissues. *J Cell Mol Med* 2010; **14**: 2702–2720.
32 Achyut BR, Yang L. Transforming growth factor-beta in the gastrointestinal and hepatic tumor microenvironment. *Gastroenterol* 2011; **141**: 1167–1178.
33 Niwa T, Tsukamoto T, Toyoda T, Mori A, Tanaka H, Maekita T *et al.* Inflammatory Processes Triggered by Helicobacter pylori Infection Cause Aberrant DNA Methylation in Gastric Epithelial Cells. *Cancer Res* 2010; **70**: 1430–1440.
34 Panning B, Jaenisch R. RNA and the epigenetic regulation of X chromosome inactivation. *Cell* 1998; **93**: 305–308.
35 Moriguchi K, Yamashita S, Tsujino Y, Tatematsu M, Ushijima T. Larger numbers of silenced genes in cancer cell lines with increased de novo methylation of scattered CpG sites. *Cancer Lett* 2007; **249**: 178–187.
36 Lauren P. The two histological main types of gastric carcinoma: diffuse and so-called intestinal-type carcinoma. An attempt at a histo-clinical classification. *Acta Pathol Microbiol Scand* 1965; **64**: 31–49.
37 Fukayama M, Hayashi Y, Iwasaki Y, Chong J, Ooba T, Takizawa T *et al.* Epstein-Barr virus-associated gastric carcinoma and Epstein-Barr virus infection of the stomach. *Lab Invest* 1994; **71**: 73–81.
38 Luo B, Wang Y, Wang XF, Liang H, Yan LP, Huang BH *et al.* Expression of Epstein-Barr virus genes in EBV-associated gastric carcinomas. *World J Gastroenterol* 2005; **11**: 629–633.
39 Cheng H, Bjerknes M, Amar J. Methods for the determination of epithelial cell kinetic parameters of human colonic epithelium isolated from surgical and biopsy specimens. *Gastroenterol* 1984; **86**: 78–85.
40 Kaneda A, Kaminishi M, Sugimura T, Ushijima T. Decreased expression of the seven ARP2/3 complex genes in human gastric cancers. *Cancer Lett* 2004; **212**: 203–210.
41 Hosoya K, Yamashita S, Ando T, Nakajima T, Itoh F, Ushijima T. Adenomatous polyposis coli 1A is likely to be methylated as a passenger in human gastric carcinogenesis. *Cancer Lett* 2009; **285**: 182–189.
42 Ho SN, Hunt HD, Horton RM, Pullen JK, Pease LR. Site-directed mutagenesis by overlap extension using the polymerase chain reaction. *Gene* 1989; **77**: 51–59.
43 Liang CC, Park AY, Guan JL. *In vitro* scratch assay: a convenient and inexpensive method for analysis of cell migration *in vitro*. *Nat Protoc* 2007; **2**: 329–333.

Supplementary Information accompanies the paper on the Oncogene website (http://www.nature.com/onc)

Carcinogenesis vol.34 no.12 pp.2833–2841, 2013
doi:10.1093/carcin/bgt309
Advance Access publication September 24, 2013

Protection from inflammatory bowel disease and colitis-associated carcinogenesis with 4-vinyl-2,6-dimethoxyphenol (canolol) involves suppression of oxidative stress and inflammatory cytokines

Jun Fang[1–3,†], Takahiro Seki[2,4,8,†], Tetsuya Tsukamoto[5], Haibo Qin[1,6], Hongzhuan Yin[1,7], Long Liao[1,6], Hideaki Nakamura[1,2] and Hiroshi Maeda[1,2,*]

[1]Research Institute for Drug Delivery System and [2]Laboratory of Microbiology and Oncology, Faculty of Pharmaceutical Sciences, Sojo University, Kumamoto 860-0082, Japan, [3]Department of Toxicology, Anhui Medical University, Hefei 230032, P. R. China, [4]Regional Cooperative Research Center, Kumamoto University, Kumamoto 861-2202, Japan, [5]Department of Diagnostic Pathology, Fujita Health University School of Medicine, Toyoake, Aichi 470-1192, Japan, [6]Department of Applied Microbiology, Sojo University, Kumamoto 860-0082, Japan and [7]Department of General Surgery, Sheng Jing Hospital, China Medical University, Shenyang 110004, P. R. China

[8]Present address: Laboratory of Angiogenesis Research, Department of Microbiology, Tumor and Cell Biology, Karolinska Institute, Nobels väg 16, SE-171 77, Stockholm, Sweden

*To whom correspondence should be addressed. Tel: +81-96-326-4114; Fax: +81-96-326-3158;
Email: hirmaeda@ph.sojo-u.ac.jp

Oxidative stress is associated with various pathological processes including inflammatory bowel disease, which is a major cause of colon cancer. Here, we examined the antioxidative and anti-inflammatory effects of 4-vinyl-2,6-dimethoxyphenol (canolol), a potent antioxidant compound obtained from crude canola oil. Oral administration of 2% dextran sulfate sodium (DSS) resulted in the progression of colitis with shortening of the large bowel length. Administering a diet containing canolol significantly suppressed pathogenesis; diarrhea markedly improved and the length of large bowel returned to almost normal. Pathological examination clearly revealed improvement of colonic ulcers. Production of inflammatory cytokines, i.e. interleukin-12 and tumor necrosis factor-α, was significantly increased during this pathological process; their production was markedly inhibited by canolol. In the azoxymethane/DSS-induced colon cancer model, mice receiving canolol had a reduced occurrence of cancer, to 60%, compared with control mice, 100% of which had colon cancer. The numbers of tumors in each mouse were also significantly reduced in mice receiving the canolol-containing diet (5.6±2.0) compared with azoxymethane/DSS control mice (10.8±4.2). No apparent toxicity of canolol was observed. Moreover, inflammatory cytokines (i.e. cyclooxygenase-2, inducible nitric oxide synthase and tumor necrosis factor-α) and oxidative responding molecules, i.e. heme oxygenase-1, in colon were suppressed during this treatment. In a mouse colon 26 solid tumor model, canolol significantly suppressed cyclooxygenase-2 expression; however, no significant tumor growth inhibition was observed, suggesting that canolol preferably shows chemopreventive effects during the stages of initiation/promotion. Canolol may, thus, be considered a potential cancer preventive agent or supplement.

Introduction

Inflammatory bowel disease (IBD) comprises a group of common diseases that manifest chronic inflammation of the colon and small intestine (1–3). The major types of IBD are Crohn's disease and ulcerative colitis. Although IBD itself is rarely fatal, it can greatly diminish the quality of life because of pain, vomiting, diarrhea and other socially unacceptable symptoms. More important, patients with IBD commonly have an increased risk of colorectal cancer, i.e. the risk of colon cancer in patients with ulcerative colitis begins to rise significantly above that of the general population approximately 8–10 years after diagnosis (1–4).

At present, a common therapeutic modality for IBD is use of anti-inflammatory agents, including sulfasalazine (Salazopyrin) and acetylsalicylic acid, steroid hormone and other immunosuppressive agents. Most of these treatments are symptomatic and palliative because the etiology of the disease is not yet established. As a result, the disease persists for a long time. Therefore, a therapeutic/preventive strategy that is based on the mechanism of IBD is an urgent necessity.

Although the exact cause of IBD must be determined, dysfunctional immunoregulation is thought to be the primary reason (1–4). Genetic, infectious, immunological, and psychological factors have also been implicated as influencing the development of IBD. Recently it was also reported that, similar to *Helicobacter pylori*-induced gastritis, bacterial infection may be involved in pathogenesis of IBD, and combination therapy with antibiotics produced a significant therapeutic effect (5–8).

Another possibility concerns reactive oxygen species (ROS): high levels were produced in IBD, which suggests that ROS may be implicated in the molecular etiology of IBD (9,10). The destructive effects of ROS on DNA, proteins and lipids, because of the highly reactive nature of ROS, may contribute to initiation and propagation of the disease (6,7). The investigation of antioxidant agents may, thus, help illuminate the etiology, treatment and prevention of IBD. Indeed, many researchers proved antioxidant treatment of IBD to be effective, not only in animal experiments but also in clinical settings (9,11).

In our laboratory, we identified a potent antioxidant phenolic compound in crude canola (rapeseed) oil, 4-vinyl-2,6-dimethoxyphenol (canolol), which exhibits a more potent alkylperoxyl ($ROO^{\bullet}$) radical scavenging activity than many well-known antioxidants, such as α-tocopherol, vitamin C, β-carotene, rutin and quercetin (12). Recently canolol was also found in mustard seed oil (13). We previously reported a strong inhibitory capacity of canolol against the endogenous mutagen peroxynitrite ($ONOO^-$), which is a potent oxidizing and nitrating agent, and suppression by canolol of bacterial mutation, via protection from DNA damage (14,15). In related studies, we demonstrated a protective effect of canolol against gastritis and gastric ulcers and a preventive effect on gastric carcinogenesis in the *H.pylori*-infected, carcinogen-treated Mongolian gerbil, which is an excellent animal model of *H.pylori*-induced, chronic active gastritis similar to IBD and involving ROS (16).

Addition of dextran sulfate sodium (DSS) to the drinking water of mice induced acute colitis characterized by bloody diarrhea, ulceration and inflammatory infiltration of leukocytes in the colon, as a result of toxicity to gut epithelial cells and distortion of the integrity of the mucosal barrier (17). The DSS-induced colitis model, which we used in this study, is commonly utilized as a model of inflammatory colitis (5,6). Application of azoxymethane (AOM) together with DSS produces a model of chronic colitis and colitis-associated colon carcinogenesis (18). The purpose of our present study was to evaluate the effectiveness of canolol for inhibition of IBD and

Abbreviations: 8-OHdG, 8-hydroxydeoxyguanosine; AOM, azoxymethane; BHT, butylated hydroxytoluene; COX-2, cyclooxygenase-2; DAI, disease activity index; DSS, dextran sulfate sodium; ELISA, enzyme-linked immunosorbent assay; HO-1, heme oxygenase-1; IBD, inflammatory bowel disease; IL-12, interleukin-12; iNOS, inducible NO synthase; LPS, lipopolysaccharide; NO, nitric oxide; ROS, reactive oxygen species; SIN-1, 3-(4-morpholinyl)sydnonimine hydrochloride; TNF-α, tumor necrosis factor-α.

†These authors contributed equally to this work.

colitis-associated carcinogenesis using a DSS-induced mouse colitis model and AOM/DSS-induced colon carcinogenesis in mice, respectively. We also investigated the effect of canolol on oxidative stress and inflammatory cytokines during development of colitis and colon carcinogenesis. The toxicity of canolol and its effect on a mouse colon 26 solid tumor model were also examined.

Material and Methods

Chemicals

Canolol (molecular weight, 180 Da), with >95% purity, was synthesized by Junsei Chemical Co., Ltd. (Tokyo, Japan). Antioxidant 2,6-di-*tert*-butyl-4-methylphenol [butylated hydroxytoluene (BHT), Sigma, St Louis, MO] was added to canolol solution (in ethanol) at the concentration of 300 ppm. BHT at this concentration had no significant therapeutic effect on colitis and colon cancer prevention (16). The preparation in solid form or solution was sealed under helium or nitrogen, and stock solution in ethanol was kept at −80°C. DSS was purchased from Wako Pure Chemical (Osaka, Japan), and AOM was from Sigma. 3-(4,5-Dimethyl-2-thiazolyl)-2,5-diphenyl-2H-tetrazolium bromide was purchased from Dojindo Chemical Laboratory (Kumamoto, Japan).

Diets

The AIN93G diet containing canolol was used in this study with some modifications. Components of the modified AIN93G diet are as follows (g/kg): corn starch, 397; casein, 200; α-corn starch, 132; sucrose, 100; soybean oil, 70; cellulose, 50; AIN93G mineral mixture, 35; AIN93G vitamin mixture, 10; L-cystine, 3.0; choline bitartrate, 2.5; and BHT, 0.014. L-Cystine and BHT were purchased from Sigma; other components were from Oriental Yeast Co., Ltd (Tokyo, Japan). Canolol was first dissolved in soybean oil and then mixed into the diet to the concentration of 0.1 or 0.3%. The control diet contained the same components but no canolol. The diets were sealed under vacuum and were stored at −30°C; they were given daily after being thawed. Each day, leftovers from the previous day's feeding were measured, and new food was provided to replace the amount eaten.

Cell culture

Human embryonic kidney cells HEK293 and human colon cancer cells Caco-2 were cultured in Dulbecco's modified Eagle's medium (Invitrogen, Carlsbad, CA), and mouse colon cancer cells colon 26 were cultured in Roswell Park Memorial Institute 1640 medium (Invitrogen), at 37°C in an atmosphere of 5% CO_2/95% air.

Animals and experimental protocol

Female ICR mice, 6 weeks old and weighing 20 to 25 g, and female BALB/c mice, 8 weeks old, were obtained from Kyudo (Tosu city, Saga, Japan). All animals were maintained under standard conditions and were fed water and murine chow *ad libitum*. All experiments were carried out according to the Guidelines of the Laboratory Protocol of Animal Handling, Sojo University, and were approved by the Animal Care Committee of Sojo University.

As to the experimental protocol for the DSS-induced colitis model, ICR mice of canolol treatment groups were fed with diet containing different concentrations of canolol during the entire experimental period (7 days). Control ICR mice were fed with the same diets but without canolol. Two hours after feeding canolol-containing diet, water containing 2% DSS was supplied to all groups except the healthy normal ICR mouse group, for entire 7 days (Supplementary Figure 1A, available at *Carcinogenesis* Online). Fresh diet was supplied daily, and the body weights of mice and amounts of consumed diet were determined each day. According to this protocol, symptoms indicating the severity of colitis obtained by macroscopic observation, such as characteristics of fecal pellets, diarrhea and hematochezia, were recorded. On day 7, the mice were killed, and specimens of blood, colon and liver were collected for biochemical and pathological examinations. After the length of each colon was measured, the colon specimen was fixed with 20% formalin solution and embedded in paraffin. Paraffin-embedded sections (6 μm thick) were prepared as usual for histological examination after hematoxylin and eosin staining, as well as for immunohistochemical staining as described below. Serum obtained from the blood collected was used to determine levels of tumor necrosis factor-α (TNF-α) and interleukin-12 (IL-12), as described below.

As to the experimental protocol for colon carcinogenesis in ICR mice induced by AOM/DSS, on day 1, AOM (at 10 mg/kg) dissolved in saline was administered intraperitoneally, and after 1 week, 2% DSS was given orally in the drinking water for 1 week. The diet was changed to the canolol-containing diet from 2 h before AOM administration and was continued for the entire experimental period of 6 weeks (Supplementary Figure 1B, available at *Carcinogenesis* Online). The amount of food consumed was calculated daily. Six weeks after the AOM injection, mice were killed, and colon and liver specimens were collected. The numbers of tumors in the colon of each mouse were measured.

Evaluation of colitis severity

We evaluated the colitis severity by measuring disease activity index (DAI) semiquantitatively, by measuring colon length as an indirect marker of inflammation, and by using histology after hematoxylin and eosin staining. The DAI was determined by scoring changes in animal weight, presence of occult blood, gross bleeding and stool consistency, as described in the literature (19). We used five grades of weight loss (0: either a gain of weight or no weight loss; 1: 1% to 5% loss; 2: 5% to 10% loss; 3: 10% to 20% loss; 4: more than 20% loss), three grades of stool consistency (0: normal; 2: loose; and 4: diarrhea) and three grades of occult blood (0: negative; 2: occult blood-positive; and 4: gross bleeding). Individual mice were graded, and the mean value for each experimental group was obtained.

Further, histological evaluation of ulcer was carried out to quantitate the degree of colitis. The numbers of ulcer regions were counted in whole-colon mucosa and divided by the total length of the evaluated colon specimens. The numbers of ulcers are expressed in unit length (mm).

Effect of canolol on colon 26 transplanted tumor

The effect of canolol on tumor was further investigated in a mouse colon cancer model. Cultured colon 26 cells (2×10^6) were implanted subcutaneously in the dorsal skin of Balb/c mice. Ten days after tumor inoculation, when tumor reached a diameter of 5–6 mm, canolol (dissolved in corn oil) was orally administration at the dose of 100 mg/kg (0.1 ml), and corn oil without canolol was used for control mice. Administration was carried out every second day, totally for three times. Growth of the tumors was monitored every 2–3 days by measuring tumor volume with a digital caliper, which was estimated by measuring longitudinal cross-section (L) and transverse section (W) according to the formula $V = (L \times W^2)/2$. On day 15 after the first canolol administration when tumor reached a diameter ~12–13 mm, mice were killed and tumor tissues were excised for histological examination and immunohistochemical analysis as described below.

Immunohistochemical analyses of cyclooxygenase-2

Expressions of cyclooxygenase-2 (COX-2) in colon mucosa of mice with DSS-induced colitis and in mice with AOM/DSS-induced colon carcinogenesis, and also in colon 26-implanted syngeneic solid tumor, were detected immunohistochemically as described previously (16), using a rabbit anti-mouse COX-2 polyclonal antibody (diluted 1:500, Cayman Chemical, Ann Arbor, MI) with 3,3′-diaminobenzidine (Wako Pure Chemical) for visualization. Images were analyzed with ImageJ software (National Institutes of Health, Bethesda, MD) for brown deposition of 3,3′-diaminobenzidine as COX-2 positive. One pathologist (T.T.) who was not informed about the samples examined the immunostained slides.

To quantitate the degree of staining, numbers of COX-2-positive cells were counted in whole-colon mucosa in DSS-induced colitis experiment, or counted in a distal quarter of colon mucosa, which is the target region of AOM/DSS in colon carcinogenesis experiment, and divided by the total length of the evaluated colon specimens to compare each sample equally. The numbers of COX-2-positive cells are illustrated in unit length (mm).

In the experiments using colon 26 solid tumor, three representative photographs were taken from each tumor using an AxioCam HRc digital camera and AxioVision v.4.8.2.0 software (Carl Zeiss, Oberkochen, Germany), and average positive areas in the each frame were compared between control and canolol groups.

Enzyme-linked immunosorbent assay for 8-hydroxydeoxyguanosine in the plasma of DSS-induced colitis mice with/without canolol treatment

Oxidative stress in the DSS-induced colitis mice with or without canolol treatment was examined by detecting 8-hydroxydeoxyguanosine (8-OHdG) in plasma, using an enzyme-linked immunosorbent assay (ELISA) kit (8-OHdG Check, JaICA, Fukuroi, Shizuoka, Japan). In brief, blood was drawn from the inferior vena cava after mice were killed, plasma samples were obtained by centrifugation (4°C, 5000*g* for 20 min) and DNA in each sample was then extracted using QuickGene DNA tissue kit (DT-S, Wako Pure Chemical), followed by hydrolysis using an 8-OHdG Assay Preparation Reagent Set (Wako Pure Chemical). The ELISA was then performed to detect 8-OHdG according to the manufacturer's instructions.

Effects of canolol on production of IL-12 and TNF-α in DSS-induced colitis

Serum samples from mice with DSS-induced colitis were obtained as described above, and levels of TNF-α and IL-12 were quantified by using an

ELISA kit (Pierce Biotechnology Rockford, IL) according to the manufacturer's instructions.

Inhibitory effect of canolol on activation of macrophages from the BALB/c mouse

Macrophages were obtained from the peritoneal fluid of mice stimulated with casein. In brief, 1 ml of 5% casein sodium (Wako Pure Chemical) in phosphate-buffered saline was injected intraperitoneally into BALB/c mice. After 3 days, mice were killed, and 5 ml of cold phosphate-buffered saline was injected into the peritoneal cavity, after which peritoneal lavage fluid (~5 ml) was collected, followed by centrifugation of the fluid (1000 r.p.m., 5 min) at 4°C. The macrophages were washed with phosphate-buffered saline three times by centrifugation, and then 15 ml of Roswell Park Memorial Institute 1640 medium (Invitrogen) with 10% FBS was added and macrophages were cultured in a plastic petri dish (100×26 mm; Nunc A/S, Roskilde, Denmark).

To activate the macrophages in culture, lipopolysaccharide (LPS) (1.0 μg/ml) and interferon-γ (0.1 μg/ml) (Sigma) were added to the cells for 24 h. Culture medium was then collected for measurement of the concentration of nitrite, which is formed from nitric oxide (NO). A significantly high amount of NO was generated by activated macrophages, which was attributable to the action of inducible NO synthase (iNOS). The nitrite concentration was quantified by using a Griess reagent kit (NO_2/NO_3 Assay Kit-C II; Dojindo Laboratories), according to the manufacturer's instructions. The production of inflammatory cytokines, i.e. TNF-α and IL-12, was also measured in culture media by using ELISA as mentioned above.

Protective effect of canolol against $ONOO^-$-induced cytotoxicity

HEK293 cells were plated at 3000 cells/well in a 96-well plate (Nunc A/S). After overnight preincubation, 1 mM or 2 mM 3-(4-morpholinyl)sydnonimine hydrochloride [SIN-1 (Dojindo Laboratories)], from which $ONOO^-$ was produced, was added to the cells. Canolol at various concentrations was then added. After an additional 48 h of incubation, cell viability was determined by using the 3-(4,5-dimethyl-2-thiazolyl)-2,5-diphenyl-2H-tetrazolium bromide (MTT) assay.

Expression of COX-2, TNF-α, iNOS and heme oxygenase-1 in colon tissues of AOM/DSS-induced carcinogenesis mice with/without feeding canolol

To examine the antioxidative, anti-inflammatory mechanisms of canolol in chemoprevention against AOM/DSS-induced colon carcinogenesis, mRNA expressions of representative oxidative inflammatory molecules [i.e. COX-2, TNF-α, heme oxygenase-1 (HO-1) and iNOS] were detected by reverse transcription–polymerase chain reaction. Briefly, after the protocol of AOM/DSS-induced carcinogenesis, total RNA from colon tissues of distal quarter in which most tumors were observed was extracted by using Sepasol®-RNA I Super reagent (NACALAI TESQUE, Kyoto, Japan), according to the manufacturer's instruction. The nucleotide sequences of the oligonucleotide primers and cycle conditions of PCR are as follows: COX-2: forward, 5′-ACA CAC TCT ATC ACT GGC ACC-3′; reverse, 5′-TTC AGG GAG AAG CGT TTG C-3′; 35 cycles of 15 s at 94°C, 15 s at 55°C and 1 min at 72°C to obtain a 274-bp cDNA; TNF-α: forward, 5′-CTA TGT CTC AGC CTC TTC TC-3′; reverse, 5′- CAG CCT TGT CCC TTG AAG AG -3′; 40 cycles of 15 s at 94°C, 30 s at 56°C and 30 s at 68°C to obtain a 353-bp cDNA; HO-1: forward, 5′-GGC CCT GGA AGA GGA GAT AG-3′; reverse, 5′-GCT GGA TGT GCT TTT GGT G-3′; 30 cycles of 30 s at 94°C, 30 s at 56°C and 30 s at 72°C to obtain a 888-bp cDNA; iNOS: forward, 5′-CCC TTC CGA AGT TTC TGG CAG CAG C-3′; reverse, 5′-GGC TGT CAG AGC CTC GTG GCT TTG G-3′; 35 cycles of 1 min at 95°C, 1 min at 65°C and 2 min at 72°C to obtain a 496-bp cDNA; GAPDH (inner control): forward, 5′-CAT GTG GGC CAT GAG GTC CAC CAC-3′; reverse, 5′-TGA AGG TCG GAG TCA ACG GAT TTG GT-3′; 30 cycles of 1 min at 94°C, 1 min at 56°C and 1 min at 72°C to obtain a 983-bp cDNA. PCR products then underwent electrophoresis on ethidium bromide-stained 1.2% agarose gels.

Safety of canolol

Female ICR mice, beginning 6 weeks of age, were fed normal diet (untreated control) or 0.3% canolol for 6 weeks. Then, mice were killed, and blood samples were obtained. Red blood cell count, white blood cell count and hemoglobin levels were determined using an automated blood counter (F-800 Microcell Counter, Toa Medical Electronics, Kobe, Japan). Plasma obtained by centrifugation was used for measurement of the liver and the kidney functions including alanine aminotransferase, aspartate aminotransferase, lactate dehydrogenase, blood urea nitrogen and total creatine using a sequential multiple Auto Analyzer system (Hitachi Ltd., Tokyo, Japan).

Statistical analyses

Data were analyzed by one-way analysis of variance followed by the Bonferroni *t*-test. Some studies with two experiments were analyzed by Mann-Whitney *U*-test, and a Fisher's exact test was used to analyze the data of tumor incidence. A difference was considered statistically significant when $P < 0.05$.

Results

Protective effect of canolol against DSS-induced colitis

Severe diarrhea accompanied by hematochezia, characterized by significant increase in DAI, was observed on day 7 in the DSS-induced colitis group without canolol; these DSS-treated mice showed a decrease in body weight though no statistical significance was found (Table I). These symptoms were markedly improved with significantly decreased DAI when canolol was added to the diet in a dose-dependent manner, and these mice showed no apparent loss of body weight (Table I). Moreover, mice with DSS-induced colitis demonstrated shortening of the large bowel, which is one of the indexes of colitis, and this pathological change was significantly improved by canolol dose dependently (Table I). No significant differences in DAI and in length of large bowel were observed in mice receiving 1% of canolol compared with normal mice (Table I), suggesting an almost complete cure of colitis. However, 1% of canolol becomes impracticable as a chemopreventive agent or supplement especially for long-term application, i.e. canolol

Table I. Protective effect of canolol against DSS-induced colitis (on day 7) and AOM/DSS-induced colon carcinogenesis (at 6 weeks)

Group	Body weight (g)	Liver weight (g)	Length of large bowel (cm)	DAI[a]
Normal	29.7±2.0	3.1±0.7	15.0±1.5**	0
DSS	26.9±4.4	2.4±0.6	9.6±2.1	9.6±0.3
DSS + 0.1% canolol	27.6±2.2	2.8±0.5	12.8±1.2*	5.2±0.7**
DSS + 0.3% canolol	28.8±3.3	2.7±0.5	13.3±2.1**#	3.7±0.6**
DSS + 1% canolol	29.3±1.5	2.9±0.1	13.7±1.7**#	1.2±1.8**#

Group	Body weight (g)	Liver weight (g)	Length of large bowel (cm)[#]	Incidence and multiplicity of tumors	
				Tumor incidence (%)[b]	Tumor multiplicity (no. of tumors/animal)
Normal	48.0±4.7	2.5±0.4	13.0±0.9**	0**	0
AOM/DSS	44.0±3.3	2.0±0.2	8.7±0.6	100	10.8±4.2
AOM/DSS + 0.1% canolol	44.6±6.1	2.1±0.1	10.9±0.9*	60**	5.3±2.7*
AOM/DSS + 0.3% canolol	44.7±1.9	2.0±0.1	10.7±0.3*	57**	5.6±2.7*

Data are means ± SD, n = 5–14 for DSS-induced colitis experiments, and n = 10–20 for AOM/DSS-induced colon carcinogenesis experiments.
[a]See text for details.
[b]Statistical significance was analyzed by Fisher's exact test.
*$P < 0.05$, **$P < 0.01$, versus the DSS control group, or versus the AOM/DSS control group.
[#]No significant difference ($P > 0.05$), versus normal group.

needs to be given more than 10 g a day in humans. Canolol at higher than 0.3% was not pursued in the carcinogenesis study and was not subjected for further investigations, i.e. pathological studies and examination of inflammatory cytokines.

Regarding the histopathology of the colon, as Figure 1 shows, the canolol-treated groups (Figure 1C and D) had much less tissue damage compared with the DSS control (Figure 1B) showing severe inflammation and erosion. Inflammation looks more alleviated in the higher dose (0.3%) group (Figure 1D) resembling normal mucosa (Figure 1A) than in the lower dose (0.1%) group (Figure 1C). After 7 days of consumption of the canolol diet, mice in both canolol groups showed significantly suppressed formation of ulcers in the colonic mucosa compared with the DSS-induced colitis group without canolol (Figure 1E).

Canolol exhibits anti-inflammatory and antioxidative activity in DSS-induced colitis

COX-2-specific immunostaining confirmed that DSS-induced colitis clearly associated with colon inflammation (Figure 2A). The COX-2 expressions in DSS control mice were significantly higher than that in normal ICR mice. However, we found the scores of COX-2 in the canolol-treated groups were reduced compared with the DSS control, though no significance was observed ($P = 0.063$).

Consistent with these findings, amount of free 8-OHdG in the plasma, that is a common index for oxidative injury of DNA, was significantly increased after DSS treatment, whereas it was suppressed dose dependently by canolol; a significant difference was observed between DSS group and DSS + 0.3% canolol group (Figure 2B).

Suppression of inflammatory cytokine production in vivo *by canolol treatment in the DSS-induced colitis model*

The anti-inflammatory tissue protective effect of canolol was further confirmed by measuring the IL-12 and TNF-α levels, which are major cytokines involved in cell killing, in the serum of mice with DSS-induced colitis. As seen in Figure 2C and D, DSS-treated mice had significantly elevated levels of both cytokines, whereas these levels decreased after treatment with canolol in a dose-dependent manner, though no significance was observed for 0.1% canolol group compared with DSS control group. This finding is consistent with the improved symptoms and pathology of colitis as noted in Table I.

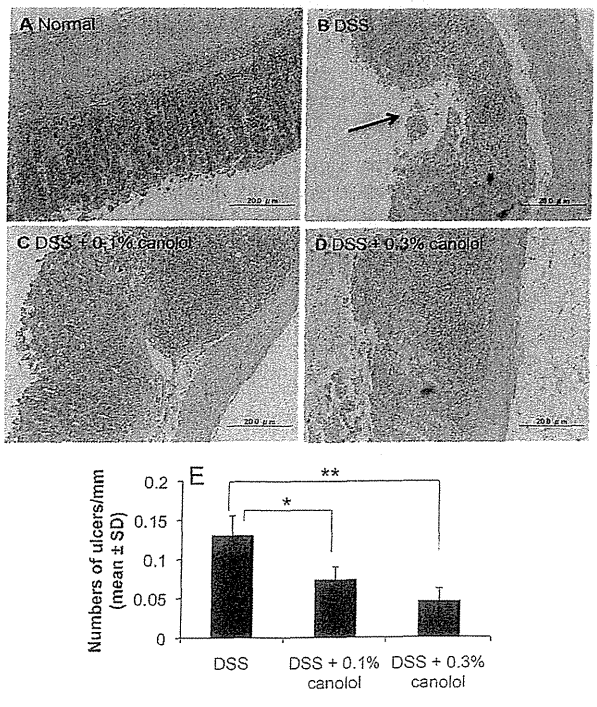

Fig. 1. Histological examination of the large bowel in DSS-induced colitis, with and without canolol treatment. (**A–D**) Hematoxylin and eosin staining of colon tissue from each experimental group. The arrow indicates the ulcer (necrosis) in the colonic mucosa. (**E**) Quantification and summary of the numbers of ulcers in each experimental group. See text for details. Data are means ± SD; $n = 6–10$. $^*P < 0.05$, $^{**}P < 0.01$.

Suppression of macrophage activation and cytokine production by canolol in vitro

The effect of canolol on the progression of inflammation as manifested by macrophage activation was investigated *in vitro* with macrophages from BALB/c mice. Canolol, at concentrations up to 200 μM, showed no apparent cytotoxicity in macrophages and human colon cancer Caco-2 cells (Supplementary Figure 2A and B, available at *Carcinogenesis* Online). Activation of macrophages was induced by simultaneously adding LPS and interferon-γ, and activation was assessed by measuring the generation of NO as nitrite (Figure 3A). Under the same conditions, when canolol was added to the cells, macrophage activation was significantly inhibited in a dose-dependent manner (Figure 3A). Moreover, canolol treatment significantly suppressed generation of inflammatory cytokines (i.e. IL-12 and TNF-α) by the macrophages (Figure 3B and C). These data clearly indicate the anti-inflammatory effect of canolol.

Protective effect of canolol against $ONOO^-$-induced cytotoxicity

Canolol is known as a compound with potent antioxidative activity, which is thought to contribute to its anti-inflammatory and cancer-preventive effects. To evaluate this, we investigated the cytoprotective effect of canolol against $ONOO^-$, which is highly cytotoxic to many cells including bacteria (14,15,20,21). $ONOO^-$ is an endogenous product of NO plus superoxide anion radical (O_2^-) in inflammatory reactions (22), and it can damage DNA, RNA, proteins and other critical molecules by means of oxidation, nitration and hydroxylation (23,24). To investigate the cytotoxicity of $ONOO^-$ and the antioxidative cytoprotection of canolol, we selected a normal cell line, human embryonic kidney cells HEK293. In this *in vitro* system, we found that ~50–60% of cells died after treatment with $ONOO^-$, which was supplied by means of a donor, SIN-1, at 1 mM (Figure 3D). Because of the short half-lives of SIN-1 (1–2 h in plasma) and $ONOO^-$ (2–3 s at physiological pH), the cytotoxicity of $ONOO^-$ in this *in vitro* culture study may be underestimated. However, the important finding is the significant inhibition of $ONOO^-$-induced cytotoxicity by canolol. In addition, a dose-dependent effect of canolol observed in HEK293 cells and the cytotoxicity of 1 mM SIN-1 was completely inhibited by 50 μM canolol (Figure 3D). In addition, canolol itself had no apparent cytotoxicity for this cell line, at least up to 100 μM (Supplementary Figure 2C, available at *Carcinogenesis* Online), which suggests that canolol is safe.

Preventive effect of canolol on AOM/DSS-induced colon carcinogenesis

Inflammatory colitis is believed to be closely associated with the occurrence of colon cancer (1–4). We, thus, investigated the preventive effect of canolol in the AOM/DSS-induced colon carcinogenesis model. The results, as shown in Table I, clearly indicated the suppressive effect of canolol on the occurrence of colon cancer. Compared with AOM/DSS control mice, 100% of which had colon tumors, ~40% of canolol-treated mice did not have these tumors. In addition, the multiplicity was significantly reduced by ~50% in the canolol-treated group compared with the untreated control group (Table I). This effect showed no clear dose dependence, as 0.1 and 0.3% canolol produced similar effect.

Suppression of COX-2, TNF-α, iNOS and HO-1 expression by canolol in AOM/DSS-induced colon carcinogenesis

To investigate the chemopreventive mechanisms of canolol, we measured mRNA expression of proinflammatory cytokines, i.e. COX-2,

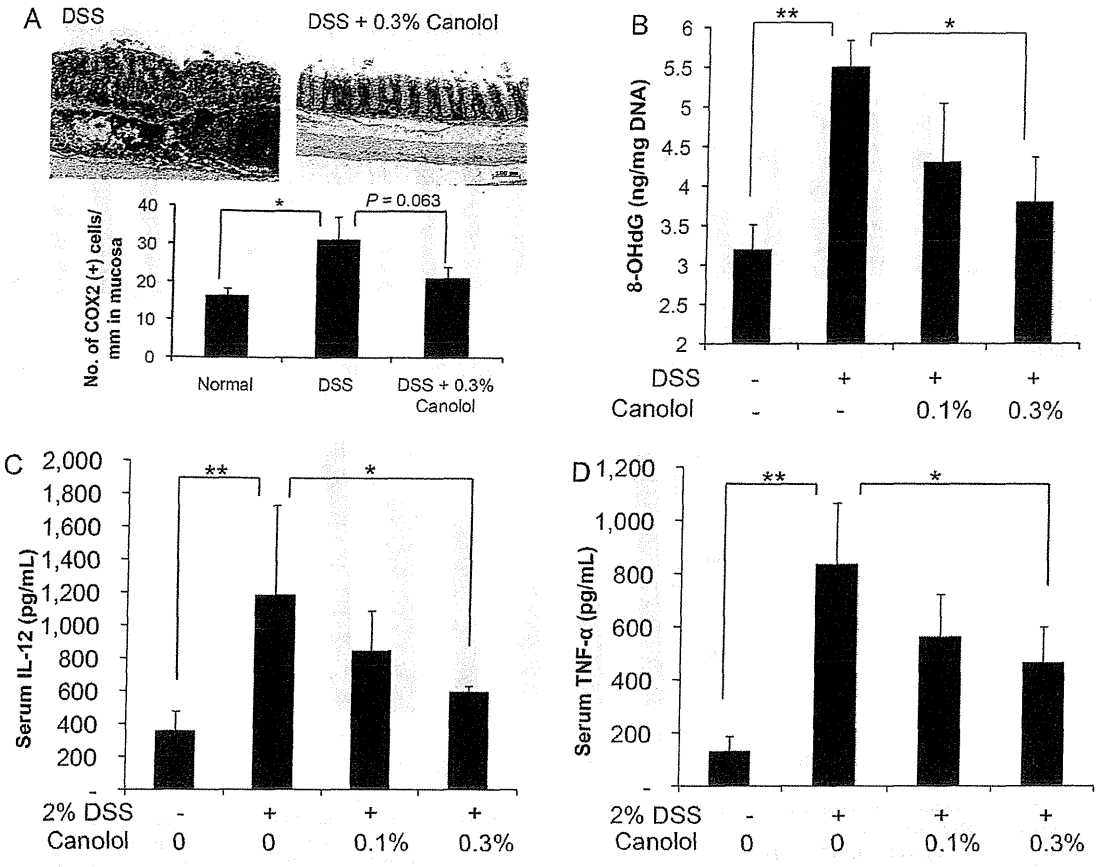

Fig. 2. Immunohistochemistry of COX-2 (**A**) in colorectal lesions, and plasma levels of 8-OHdG (**B**), as well as production of IL-12 (**C**) and TNF-α (**D**) in DSS-induced colitis and the protective effect of canolol. The protocols of DSS-induced colitis and canolol treatment are presented in Figure 1. Seven days after the start of DSS administration, mice were killed and serum samples were collected for measuring IL-12 and TNF-α by means of ELISA. See text for details. Data are means ± SD ($n = 6$–10). $^{*}P < 0.05$, $^{**}P < 0.01$.

TNF-α and iNOS in AOM/DSS-induced colon carcinogenesis. Similar to the findings in DSS colitis experiments (Figure 2A and D), significant decreases of TNF-α and iNOS expression were observed (Figure 4B and C). As to COX-2, though no significance was observed ($P = 0.054$), apparent lowered expression was found after feeding 0.3% of canolol (Figure 4A), and further immunohistochemical staining of COX-2 in colon mucosa also showed that average number of COX-2-positive cells in unit length tended to be lower at 0.46±0.31/mm in canolol group compared with 0.89±0.39/mm in AOM/DSS control group, although without statistical significance (data are mean ± SD; $P = 0.082$, Mann–Whitney U-test) (Figure 4E).

Moreover, when we examined the expression of HO-1, a major antioxidative antiapoptotic molecule in various tumors reflecting oxidative and other cellular stresses (25), a significantly decreased expression was observed in canolol group compared with AOM/DSS control group (Figure 4D), which in part supported the antioxidative effect of canolol, i.e. higher oxidative levels in AOM/DSS group inducing higher expression of HO-1, whereas suppressed oxidative stress by canolol resulted in lower expression of HO-1.

Effect of canolol on colon 26 solid tumor model

To further examine the effect of canolol on tumor growth, a syngeneic mouse colon tumor model (colon 26) was used. After oral administration of canolol (100 mg/kg) for three times, COX-2 expressions in tumors were significantly lowered (Figure 4F): average area of COX-2 was 1.42±0.47% in the control (no canolol) group, whereas 0.215±0.072% in the group fed with 0.3% canolol (data are mean ± SD; $P < 0.002$, Mann–Whitney U-test). However, only a slight but no significant suppression of tumor growth was found (Supplementary Figure 3, available at *Carcinogenesis* Online).

Safety of canolol

As summarized in Table II, no significant adverse effects such as decreases in red blood cell and white blood cell counts and hemoglobin levels were found in ICR mice after feeding 0.3% canolol for 6 weeks, which is the same dose for preventing AOM/DSS-induced colon carcinogenesis. Also, no significant changes in the liver enzymes and kidney functions were found under the same conditions.

Discussion

In this study, we demonstrated the protective effect of canolol, a potent antioxidant that was recently isolated from canola (rapeseed) oil (12), on IBD in a DSS-induced mouse model. Oral administration of a diet containing canolol to the mice significantly reduced the symptoms and suppressed the progression of this disease, as supported by the lengthening of the large bowel (Table I), as well as by reduced severity and numbers of ulcers in the colonic mucosa (Figure 1) and lower levels of COX-2 expression and inflammatory cytokines (Figure 2A, C and D). These findings were associated with a decreased occurrence of colon carcinogenesis induced by AOM/DSS (Table I). However, though suppression of COX-2 expression by canolol was also found in colon 26 solid tumor (Figure 4F), no significant delay of tumor growth was observed (Supplementary Figure 3,

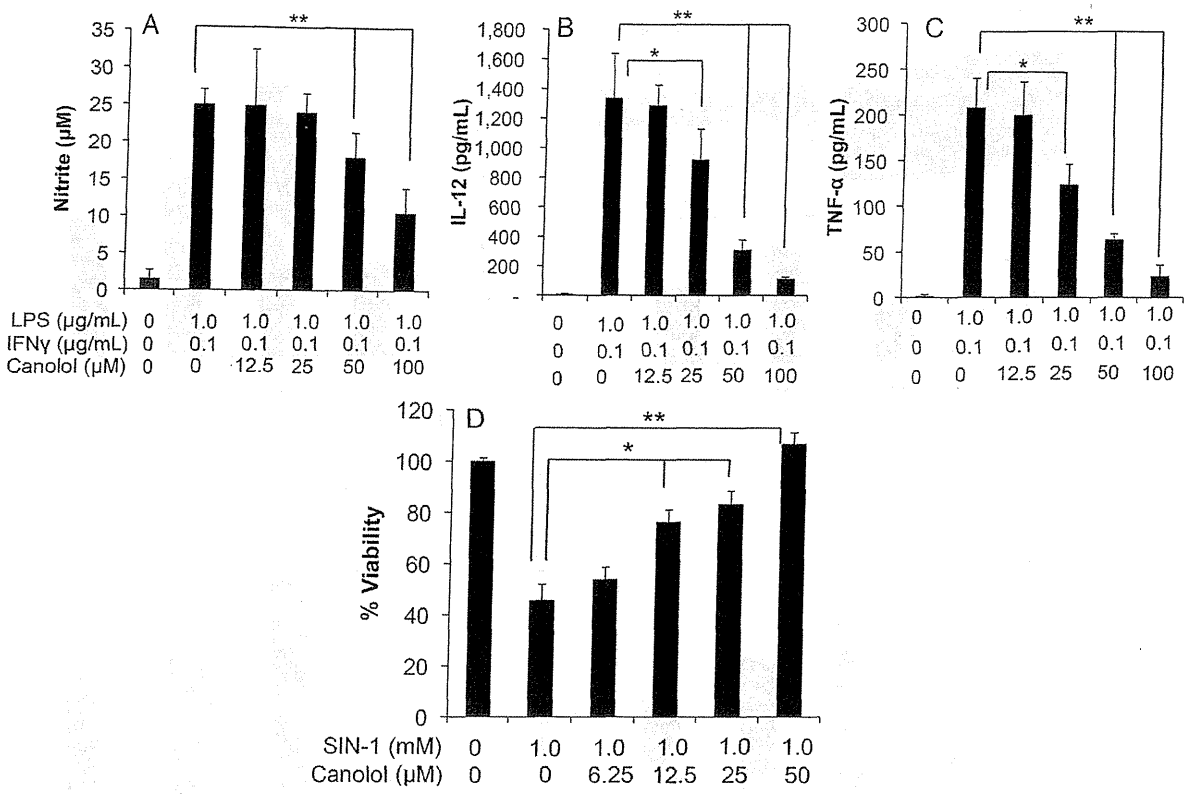

Fig. 3. Suppression of macrophage activation (**A**) and subsequent generation of IL-12 (**B**) and TNF-α (**C**), and cytoprotective effect against the toxicity of peroxynitrite ($ONOO^-$) in HEK293 (**D**) by canolol. Mouse macrophages were obtained from BALB/c mice. Macrophage activation, as generation of NO, was evaluated by using a Griess Reagent kit. IL-12 and TNF-α were measured using ELISA. See text for details. For cytotoxicity study, 3000 cells/well were plated in a 96-well plate. After overnight preincubation, 1 mM SIN-1 ($ONOO^-$ donor) was added to the cells. Different concentrations of canolol were administered. After an additional 48 h of incubation, cell viability was determined by using the 3-(4,5-dimethyl-2-thiazolyl)-2,5-diphenyl-2H-tetrazolium bromide (MTT) assay. Data are means ± SD ($n = 6–8$). $^*P < 0.05$, $^{**}P < 0.01$.

available at *Carcinogenesis* Online). Partly consistent with these findings, canolol does not show apparent cytotoxicity against cultured cells including colon cancer cells Caco-2 (Supplementary Figure 2, available at *Carcinogenesis* Online). These data suggested that canolol might not exhibit chemotherapeutic/cytotoxic effect against the growing tumors, whereas it exhibited significant chemopreventive effect probably during the stages of initiation and/or promotion via its antioxidative and anti-inflammatory activities.

Part of this anti-inflammatory effect of canolol may be attributable to its antioxidative or scavenging activity against the excess ROS that are produced during inflammation. ROS are known to be involved in many diseases including inflammation, infections, ischemia/reperfusion injury, neurological disorders, Parkinson's disease, hypertension and cancer (26–28). During the process of inflammation, O_2^- is extensively produced in infiltrated neutrophils and activated macrophages by means of reduced nicotinamide adenine dinucleotide phosphate oxidase and probably even more by xanthine oxidase, which is highly expressed in inflamed tissues (27–30). We described similar results in our previous study with an influenza virus infection model (29,31) and in our more recent study with a xanthine oxidase inhibitor in a rat liver ischemia/reperfusion model (30). Excess generation of ROS was also observed in DSS-induced colitis model and could be suppressed by xanthine oxidase inhibitor (Fang,J., Yin,H.Z., Liao,L., Qin,H.B., Ueda,F., Uemura,K., Eguchi,K., Bharate,G.Y., Nakamura,H., and Maeda,H., unpublished data). O_2^- is then converted to hydrogen peroxide by superoxide dismutase and/or glutathione peroxide, after which the hydrogen peroxide is converted to hydroxyl radicals in the presence of transition metals (e.g. Fe^{2+}). A massive amount of NO is also generated by iNOS that is upregulated in activated macrophages (22,28), and NO can react rapidly with O_2^- to form the more toxic species $ONOO^-$. All of these highly reactive biological radicals readily cross cell membranes and react with proteins, DNA and lipids (23,24,32–34), which results in cell damage. Furthermore, removal of NO by reaction with O_2^- on the vascular endothelial surface causes vasoconstriction and triggers neutrophil adherence and accumulation, which will promote the pathological process of inflammation (20,21). This notion is supported by results of the present study, in which canolol treatment significantly protected cells against the toxicity of $ONOO^-$ (Figure 4D and E), and moreover it also significantly decreased the levels of 8-OHdG, one of the major indicators of oxidative stress, in DSS-induced colitis model (Figure 2B).

Moreover, it was also reported that the antioxidative and cytoprotective effect of canolol is probably partly through upregulating antioxidative molecules such as NF-E2-related factor, HO-1, catalase and glutathione S-transferase-pi via an extracellular signal-regulated kinase-mediated pathway (35). However, in this study we found the decrease of HO-1 expression in the distal quarter of the colon where tumors occurred most frequently (Figure 4D). This finding may indicate the different expression profile of HO-1 in normal tissues and tumor tissues. In normal tissues, upregulated HO-1 protects against oxidative stress and other damages, whereas many tumors highly express HO-1 to support their rapid growth and protect against various oxidative stresses (25). Moreover, these findings partly agreed with a recent report showing that HO-1 may protect healthy tissues against carcinogen-induced injury, but in already growing tumors, it seems to favor their progression toward more malignant forms (36).

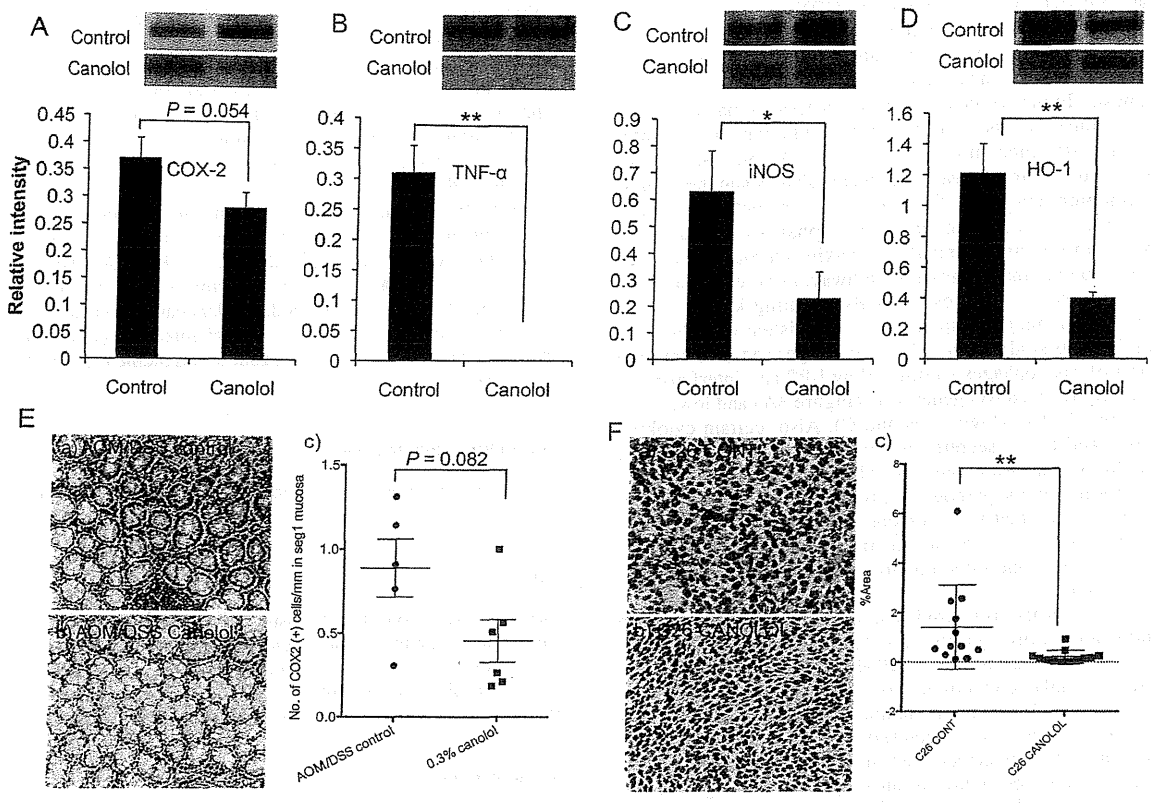

Fig. 4. Suppression of COX-2 (**A**), TNF-α (**B**) and iNOS (**C**) and upregulation of HO-1 by canolol as evaluated by reverse transcription–polymerase chain reaction, and the decreased COX-2 expression in colon tissue of AOM/DSS-treated ICR mice (**E**) and colon 26 (C26) mouse tumor (**F**) *in vivo* after canolol treatment. In (**A–D**), two representative DNA bands of each group (control and canolol group) are shown, and the results were semiquantitated as relative intensity compared with the intrinsic DNA expression of GAPDH as control. Immunohistochemical staining of COX-2 in colon tissue of AOM/DSS control mice (E-a) and canolol-treated mice (E-b) is shown in (E), and that in C26 tumor tissues without and with canolol treatment is shown in (F-a) and (F-b), respectively; in both cases, the COX-2-positive (brown colored) area was quantitated (E-c and F-c). See text for details. Data are means ± SD ($n = 5–12$). $^{*}P < 0.05$, $^{**}P < 0.01$ by Mann–Whitney *U*-test.

Table II. Change in RBC, WBC, hemoglobin and plasma liver enzyme levels and kidney function after feeding canolol (0.3% for 6 weeks) in ICR mice[a]

	RBC (10^4/μl)		WBC (10^2/μl)		Hb (g/dl)
Normal	992.2±35.9		30.4±4.2		16.0±0.6
Canolol[b]	953.0±20.2		28.8±1.9		15.1±0.4
	BUN (mg/dl)	Cr (mg/dl)	AST (IU/l)	ALT (IU/l)	LDH (IU/l)
Normal	20.7±0.8	0.15±0.02	67.3±2.8	28.4±2.2	1383.0±54.7
Canolol[b]	21.5±1.3	0.13±0.01	65.1±4.5	37.6±4.2	1036.4±149.3

ALT, alanine aminotransferase; AST, aspartate aminotransferase; BUN, blood urea nitrogen; Cr, creatinine; Hb, hemoglobin; LDH, lactate dehydrogenase; RBC, red blood cells; WBC, white blood cells.
[a]No significant difference was found between canolol feeding mice and normal mice in all selected indices. Values are presented as means ± SE. $n = 5–8$.
[b]Canolol was administered at 0.3% (w/w) in diet. Assays were carried out at 6 weeks after feeding canolol.

Taken together, the association of canolol with HO-1 in AOM/DSS colon carcinogenesis seems to be different from that in normal tissues during stresses and damages as described earlier (35); further investigations are thus warranted to make clear the mechanisms involved in the effect of canolol in different conditions.

COX-2 is the enzyme that catalyzes the conversion of arachidonic acid to prostaglandins, it is unexpressed under normal conditions in most cells, but elevated levels are found under inflammatory condition and is thus largely responsible for causing inflammation (37). Many studies revealed that the products of COX-2 prostaglandins are highly involved in the carcinogenesis of many tumors including colorectal cancer metastasis and tongue and esophageal cancers (38,39). In this study, we found a decrease in COX-2 expression (both in mRNA and protein levels) after canolol treatment, though not statistically significant, in DSS-induced colitis (Figure 2A) and in AOM/DSS-induced colon carcinogenesis (Figure 4A). These findings at least partly suggested that suppression of COX-2 expression is probably involved in the effect of canolol on DSS-induced colitis and colon carcinogenesis.

Both the present study and our previous study (16) of canolol *in vivo* showed suppression of a number of inflammatory mediators

such as TNF-α, IL-12, IL-1β, iNOS and COX-2 (Figure 2A, C, and D, Figure 4A–C and ref. 16), which confirms that this suppression will contribute to the anti-inflammatory activity and the antioxidative effect of canolol against IBD and the subsequent colon carcinogenesis. Infiltrated neutrophils and activated macrophages are major producers of these inflammatory cytokines during inflammatory diseases including IBD (40,41). ROS play an important initial role in both the activation of macrophages and the induction of inflammatory cytokines. Bulua et al. (42) recently reported that ROS are crucial in LPS-stimulated macrophages for inducing production of several proinflammatory cytokines through an mitogen-activated protein kinase signaling pathway, as an essential feature of innate immunity. Apoptosis signal-regulating kinase 1 is also involved in this immune response (43). Consistent with this result, we found in this study that the ROS scavenger canolol suppressed activation of macrophages stimulated by LPS and interferon-γ, as evidenced by reduced NO generation (Figure 3A) and lower levels of IL-12 and TNF-α (Figure 3B and C). Also, certain cytokines, i.e. TNF-α and IL-12, secreted by activated phagocytic cells, can enhance ROS generation (44,45), which explains the important role of cytokines in the pathogenic process of inflammation. These findings suggested that the chemopreventive effect of canolol is mostly via its antioxidative and anti-inflammatory effect to inhibit the oxidative stress and inflammation, thus inhibiting the carcinogenesis cascades.

Canolol is extracted from crude canola oil after roasting the rape seeds and is a naturally occurring compound in this edible oil whose concentration is estimated to be ~220–1200 ppm (12), which could provide doses similar to that used in our study. The amounts of canolol administered orally in the diet in this study were 0.1% and 0.3%, or equivalent to 1–3 g/kg (dry weight) of feed for humans, which is a reasonable range for supplement diet. In our previous study, we also applied the 0.1% concentration in an *H.pylori*-induced gastric carcinogenesis model and showed a significant cancer-preventive effect (15). Because the present colon carcinogenesis prevention study revealed no dose dependency (Table I), the 0.1% canolol concentration may be the level of saturation. That is, 0.1% canolol may be sufficient to prevent colon carcinogenesis.

Furthermore, canolol showed very little cytotoxicity to cells in culture: it had no apparent toxicity in human HEK293 cells at least up to 100 μM, in human Caco-2 cells up to 200 μM (Supplementary Figure 2B and C, available at *Carcinogenesis* Online) or in macrophages up to 300 μM (0.054 mg/ml), as described previously (16) and in present study (Supplementary Figure 2A, available at *Carcinogenesis* Online), which is a far higher concentration than the concentration for effective scavenging of ROS (i.e. 1–20 μM) (12,46). Similar results were obtained in our *in vivo* study. Mice receiving a diet containing canolol up to 0.3% for 6 weeks showed no apparent change in body weight (Table II) and no apparent toxicity as reflected by blood cell count and biochemistry of liver and kidney functions (Table II). This safety profile suggests that canolol has the potential to be not only a drug but also a food supplement for disease prevention.

Colon cancer is the most common type of cancer in developed countries, with the highest incidence and mortality rates (47). With regard to the mechanisms of colon carcinogenesis, genetic factors seem to play an important role, as in familial adenomatous polyposis (48). However, ROS were recently found to be one of the critical factors in colon carcinogenesis and in familial adenomatous polyposis (49). Dietary habits are known to be highly associated with the occurrence of colon cancer (50,51). For example, oxidized oils in high-fat diets, which are a risk factor for colon cancer, generate lipid peroxyl radicals in the presence of heme or iron, damage DNA and consequently induce colon cancer (50). Also, ROS contribute to many conditions other than inflammation, such as virus infections and ischemia/reperfusion injury, as described above.

Moreover, an unhealthy diet, with a low consumption of green vegetables and thus less antioxidants, may lead to the adverse consequences of these ROS-related diseases. It should be noted that purified canola oil that is available in large supermarkets does not contain canolol because the refining process removes it (12). It should be also noted that the content of canolol increases dramatically by roasting process as used in traditional oil refining process (12). Thus, the refining process should be modified so that canolol is retained. The canolol used in this study was synthesized, so synthetic canolol may be used as a preventive agent for these diseases.

For IBD treatment, drugs commonly used in clinical settings provide symptomatic or palliative relief. Canolol treatment, however, aims more at the cause of the disease, i.e. ROS. All these data therefore suggest that canolol may be effective not only for IBD-associated colon cancer but also for ROS-dependent carcinogenesis, as described for gastric cancer involving *H.pylori* infection (16). Canolol thus holds promise as a preventive agent or supplement for both IBD and colon cancer.

Supplementary material

Supplementary Figures 1–3 can be found at http://carcin.oxfordjournals.org/

Funding

Grants-in-Aid from the Ministry of Education, Science, Culture, Sports and Technology of Japan (No. 08011717); Cancer Speciality grant from the Ministry of Health, Welfare and Labour (H23-3rd Cancer Project-General-001); research funds of the Faculty of Pharmaceutical Sciences at Sojo University (RW15000025).

Acknowledgements

The authors thank Ms Masayo Idenoue for her excellent technical assistance.

Conflict of Interest Statement: None declared.

References

1. Baumgart,D.C. *et al.* (2007) Inflammatory bowel disease: cause and immunobiology. *Lancet*, **369**, 1627–1640.
2. Baumgart,D.C. *et al.* (2007) Inflammatory bowel disease: clinical aspects and established and evolving therapies. *Lancet*, **369**, 1641–1657.
3. Xavier,R.J. *et al.* (2007) Unravelling the pathogenesis of inflammatory bowel disease. *Nature*, **448**, 427–434.
4. Khor,B. *et al.* (2011) Genetics and pathogenesis of inflammatory bowel disease. *Nature*, **474**, 307–317.
5. Ohkusa,T. *et al.* (2004) The role of bacterial infection in the pathogenesis of inflammatory bowel disease. *Intern. Med.*, **43**, 534–539.
6. Arthur,J.C. *et al.* (2012) Intestinal inflammation targets cancer-inducing activity of the microbiota. *Science*, **338**, 120–123.
7. Ohkusa,T. *et al.* (2005) Effectiveness of antibiotic combination therapy in patients with active ulcerative colitis: a randomized, controlled pilot trial with long-term follow-up. *Scand. J. Gastroenterol.*, **40**, 1334–1342.
8. Ohkusa,T. *et al.* (2010) Newly developed antibiotic combination therapy for ulcerative colitis: a double-blind placebo-controlled multicenter trial. *Am. J. Gastroenterol.*, **105**, 1820–1829.
9. Rezaie,A. *et al.* (2007) Oxidative stress and pathogenesis of inflammatory bowel disease: an epiphenomenon or the cause? *Dig. Dis. Sci.*, **52**, 2015–2021.
10. Pavlick,K.P. *et al.* (2002) Role of reactive metabolites of oxygen and nitrogen in inflammatory bowel disease. *Free Radic. Biol. Med.*, **33**, 311–322.
11. Yukitake,H. *et al.* (2011) BTZO-15, an ARE-activator, ameliorates DSS- and TNBS-induced colitis in rats. *PLoS One*, **6**, e23256.
12. Wakamatsu,D. *et al.* (2005) Isolation, identification, and structure of a potent alkyl-peroxyl radical scavenger in crude canola oil, canolol. *Biosci. Biotechnol. Biochem.*, **69**, 1568–1574.
13. Shrestha,K. *et al.* (2012) Isolation and identification of a potent radical scavenger (canolol) from roasted high erucic mustard seed oil from Nepal and its formation during roasting. *J. Agric. Food Chem.*, **60**, 7506–7512.

14. Kuwahara,H. *et al.* (2004) Antioxidative and antimutagenic activities of 4-vinyl-2,6-dimethoxyphenol (canolol) isolated from canola oil. *J. Agric. Food Chem.*, **52**, 4380–4387.
15. Kuwahara,H. *et al.* (2009) Generation of drug-resistant mutants of *Helicobacter pylori* in the presence of peroxynitrite, a derivative of nitric oxide, at pathophysiological concentration. *Microbiol. Immunol.*, **53**, 1–7.
16. Cao,X. *et al.* (2008) 4-Vinyl-2,6-dimethoxyphenol (canolol) suppresses oxidative stress and gastric carcinogenesis in *Helicobacter pylori*-infected carcinogen-treated Mongolian gerbils. *Int. J. Cancer*, **122**, 1445–1454.
17. Wirtz,S. *et al.* (2007) Chemically induced mouse models of intestinal inflammation. *Nat. Protoc.*, **2**, 541–546.
18. Neufert,C. *et al.* (2007) An inducible mouse model of colon carcinogenesis for the analysis of sporadic and inflammation-driven tumor progression. *Nat. Protoc.*, **2**, 1998–2004.
19. Takagi,T. *et al.* (2011) Carbon monoxide liberated from carbon monoxide-releasing molecule exerts an anti-inflammatory effect on dextran sulfate sodium-induced colitis in mice. *Dig. Dis. Sci.*, **56**, 1663–1671.
20. Akaike,T. *et al.* (2000) Nitric oxide and virus infection. *Immunology*, **101**, 300–308.
21. Beckman,J.S. *et al.* (1996) Nitric oxide, superoxide, and peroxynitrite: the good, the bad, and ugly. *Am. J. Physiol.*, **271**(5 Pt 1), C1424–C1437.
22. Akaike,T. *et al.* (1996) Pathogenesis of influenza virus-induced pneumonia: involvement of both nitric oxide and oxygen radicals. *Proc. Natl Acad. Sci. USA*, **93**, 2448–2453.
23. Niles,J.C. *et al.* (2006) Peroxynitrite-induced oxidation and nitration products of guanine and 8-oxoguanine: structures and mechanisms of product formation. *Nitric Oxide*, **14**, 109–121.
24. Sawa,T. *et al.* (2006) Nitrative DNA damage in inflammation and its possible role in carcinogenesis. *Nitric Oxide*, **14**, 91–100.
25. Fang,J. *et al.* (2004) Antiapoptotic role of heme oxygenase (HO) and the potential of HO as a target in anticancer treatment. *Apoptosis*, **9**, 27–35.
26. McCord,J.M. (2000) The evolution of free radicals and oxidative stress. *Am. J. Med.*, **108**, 652–659.
27. Maeda,H. *et al.* (1991) Oxygen free radicals as pathogenic molecules in viral diseases. *Proc. Soc. Exp. Biol. Med.*, **198**, 721–727.
28. Maeda,H. *et al.* (1998) Nitric oxide and oxygen radicals in infection, inflammation, and cancer. *Biochemistry (Mosc).*, **63**, 854–865.
29. Akaike,T. *et al.* (1990) Dependence on O2- generation by xanthine oxidase of pathogenesis of influenza virus infection in mice. *J. Clin. Invest.*, **85**, 739–745.
30. Fang,J. *et al.* (2010) Tissue protective effect of xanthine oxidase inhibitor, polymer conjugate of (styrene-maleic acid copolymer) and (4-amino-6-hydroxypyrazolo[3,4-*d*]pyrimidine), on hepatic ischemia-reperfusion injury. *Exp. Biol. Med. (Maywood)*, **235**, 487–496.
31. Oda,T. *et al.* (1989) Oxygen radicals in influenza-induced pathogenesis and treatment with pyran polymer-conjugated SOD. *Science*, **244**, 974–976.
32. Davies,K.J. (1993) Protein modification by oxidants and the role of proteolytic enzymes. *Biochem. Soc. Trans.*, **21**, 346–353.
33. Lindahl,T. (1993) Instability and decay of the primary structure of DNA. *Nature*, **362**, 709–715.
34. Wagner,B.A. *et al.* (1994) Free radical-mediated lipid peroxidation in cells: oxidizability is a function of cell lipid bis-allylic hydrogen content. *Biochemistry*, **33**, 4449–4453.
35. Dong,X. *et al.* (2011) Protective effect of canolol from oxidative stress-induced cell damage in ARPE-19 cells via an ERK mediated antioxidative pathway. *Mol. Vis.*, **17**, 2040–2048.
36. Was,H. *et al.* (2011) Effects of heme oxygenase-1 on induction and development of chemically induced squamous cell carcinoma in mice. *Free Radic. Biol. Med.*, **51**, 1717–1726.
37. Dubois,R.N. *et al.* (1998) Cyclooxygenase in biology and disease. *FASEB J.*, **12**, 1063–1073.
38. Hawcroft,G. *et al.* (2012) The omega-3 polyunsaturated fatty acid eicosapentaenoic acid inhibits mouse MC-26 colorectal cancer cell liver metastasis via inhibition of PGE2-dependent cell motility. *Br. J. Pharmacol.*, **166**, 1724–1737.
39. Miyamoto,S. *et al.* (2008) A novel rasH2 mouse carcinogenesis model that is highly susceptible to 4-NQO-induced tongue and esophageal carcinogenesis is useful for preclinical chemoprevention studies. *Carcinogenesis*, **29**, 418–426.
40. Nathan,C. (2006) Neutrophils and immunity: challenges and opportunities. *Nat. Rev. Immunol.*, **6**, 173–182.
41. Mosser,D.M. *et al.* (2008) Exploring the full spectrum of macrophage activation. *Nat. Rev. Immunol.*, **8**, 958–969.
42. Bulua,A.C. *et al.* (2011) Mitochondrial reactive oxygen species promote production of proinflammatory cytokines and are elevated in TNFR1-associated periodic syndrome (TRAPS). *J. Exp. Med.*, **208**, 519–533.
43. Matsuzawa,A. *et al.* (2005) ROS-dependent activation of the TRAF6-ASK1-p38 pathway is selectively required for TLR4-mediated innate immunity. *Nat. Immunol.*, **6**, 587–592.
44. Warren,J.S. *et al.* (1988) Macrophage-derived cytokines amplify immune complex-triggered O2-. responses by rat alveolar macrophages. *Am. J. Pathol.*, **130**, 489–495.
45. Szefler,S.J. *et al.* (1989) IFN-gamma and LPS overcome glucocorticoid inhibition of priming for superoxide release in human monocytes. Evidence that secretion of IL-1 and tumor necrosis factor-alpha is not essential for monocyte priming. *J. Immunol.*, **142**, 3985–3992.
46. Galano,A. *et al.* (2011) Canolol: a promising chemical agent against oxidative stress. *J. Phys. Chem. B*, **115**, 8590–8596.
47. Jemal,A. *et al.* (2010) Global patterns of cancer incidence and mortality rates and trends. *Cancer Epidemiol. Biomarkers Prev.*, **19**, 1893–1907.
48. Strate,L.L. *et al.* (2005) Hereditary colorectal cancer syndromes. *Cancer Causes Control*, **16**, 201–213.
49. Ullman,T.A. *et al.* (2011) Intestinal inflammation and cancer. *Gastroenterology*, **140**, 1807–1816.
50. Sawa,T. *et al.* (1998) Lipid peroxyl radicals from oxidized oils and heme-iron: implication of a high-fat diet in colon carcinogenesis. *Cancer Epidemiol. Biomarkers Prev.*, **7**, 1007–1012.
51. Chao,A. *et al.* (2005) Meat consumption and risk of colorectal cancer. *JAMA*, **293**, 172–182.

Received December 13, 2012; revised July 8, 2013; accepted July 23, 2013

Anticancer effects of 4-vinyl-2,6-dimethoxyphenol (canolol) against SGC-7901 human gastric carcinoma cells

JING JIANG[1], DONG-HUI CAO[1], TETSUYA TSUKAMOTO[2], GUO-QING WANG[3], ZHI-FANG JIA[1], JIAN SUO[4] and XUE-YUAN CAO[4]

[1]Division of Clinical Epidemiology, First Hospital of Jilin University, Changchun, Jilin 130021, P.R. China;
[2]Division of Pathology, School of Medicine, Fujita Health University, Toyoake, Japan;
[3]Department of Pathogeny Biology, Norman Bethune Medical College of Jilin University;
[4]Department of Gastric and Colorectal Surgery, First Hospital of Jilin University, Changchun, Jilin 130021, P.R. China

Received December 12, 2012; Accepted February 27, 2013

DOI: 10.3892/ol.2013.1230

Abstract. Gastric cancer remains the fourth most commonly diagnosed cancer and is the second leading cause of cancer-related mortality worldwide. The aim of this study was to investigate the effects of canolol on the proliferation and apoptosis of SGC-7901 human gastric cancer cells and its relevant molecular mechanisms. The 3-(4,5-dimethylthiazol-2-yl)-2,5-diphenyltetrazolium bromide (MTT) assay was used to observe the effect of canolol on the proliferation of SGC-7901 human gastric adenocarcinoma cells. The results showed that SGC-7901 cells exhibited a marked dose-dependent reduction in the proliferation rate. The survival rate of the cells was 88.86±1.58% at 50 μmol/l, decreasing to 53.73±1.51% at 800 μmol/l ($P<0.05$). By contrast, canolol had no significant toxicity on the human gastric mucosal epithelial cell line GES-1. The vivid images of cell morphology using an inverted microscope provided confirmation of the MTT assay. Treatment of SGC-7901 cells with canolol resulted in apoptosis demonstrated by flow cytometry. Furthermore, canolol downregulated the mRNA levels of COX-2, but had no significant effect on the mRNA expession of the Bax and Bcl-2 genes. These findings suggest that canolol has potential to be developed as a new natural anti-gastric carcinoma agent.

Introduction

Gastric cancer remains the fourth most commonly diagnosed cancer and is the second leading cause of cancer related mortality worldwide (1). Gastric cancer is the most common cancer in Eastern Asia (2). Eradication of *H. pylori* in the stomach by administration of oral antimicrobial agents results in the resolution of *H. pylori*-infected chronic active gastritis and significantly reduces the risk of gastric cancer development (3). However, bacterial eradication treatment has been lacking. The occurrence of antibiotic-resistant *H. pylori* has been reported (4) and is occasionally associated with adverse effects. Regular therapies such as chemotherapy, biotherapy and radiotherapy have been previously applied, however, they have unavoidable side effects (5). Therefore, more effective alternative approaches for gastric cancer prevention and therapies without undesirable side-effects are needed.

It is widely accepted that phytochemical, especially phenolic, compounds are associated with anticancer effects by affecting molecular events in the initiation, promotion and progression stages. Recent studies have demonstrated protective effects of plant phenolic compounds against gastric cancer (6-8). The expansion ability of tumor cells depends on the rate of both cell proliferation and cell apoptosis. The particular features of tumor cells allow them to evade apoptosis, a cell suicide program that reduce the damaged or mutated cells to maintain homeostasis (9).

Canolol, 4-vinyl-2,6-dimethoxyphenol (Fig. 1), is purified from crude canola oil and is a novel and potent antioxidant. Canolol has been proven to prevent *H. pylori*-induced gastritis and carcinogenesis in an animal model (10). However, its potential anti-proliferative and proapoptotic effects on gastric cancer cells and the possible mechanisms remain unknown.

The role of cyclooxygenase-2 (COX-2) inhibitors in the chemoprophylaxis of gastric cancer has been investigated. COX-2, the inducible isoform of COX, is undetectable in normal tissues and highly expressed in gastric tumors (11). Experimental studies have identified the correlation between COX-2 overexpression and the increased cell proliferation and decreased cell apoptosis in malignant tumor cells (12,13). COX inhibitors (Coxibs) are a series of drugs with analgesic, antipyretic and anti-inflammatory properties. Evidence suggests that COX-2 inhibitors correlate with tumor inhibition in breast (14) and endometrial cancer cell lines (15). Induction of apoptosis has increasingly become important with regard to the mechanism of cancer defense and prevention (16). However, the involvement of COX-2 inhibitors in gastric cancer prophy-

Correspondence to: Dr Xue-Yuan Cao, Department of Gastric and Colorectal Surgery, First Hospital of Jilin University, Changchun, Jilin 130021, P.R. China
E-mail: ccmzc32jdyycao@yahoo.com.cn

Key words: canolol, gastric cancer, COX-2, anti-proliferation, apoptosis

laxis remains to be determined, as the long-term use of COX-2 inhibitors exerts side-effects on the cardiovascular system and the digestive tract. A possible correlation between COX-2 inhibition and cell apoptosis in gastric cancer cell lines has yet to be examined.

In the present study, the effects of canolol on growth and apoptosis of human gastric adenocarcinoma SGC-7901 cells were investigated. Human gastric mucosal epithelial (GES-1) cells were used as the control cell model to examine the non-specific cytotoxicity of canolol. The mRNA expression levels of COX-2, Bcl-2 and Bax were detected to further elucidate the possible mechanisms involved.

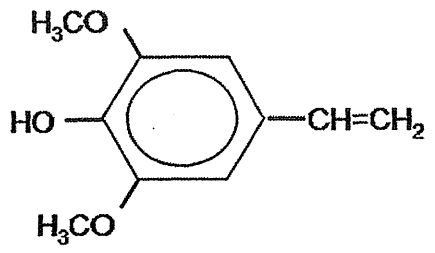

Figure 1. Chemical structure of canolol, 4-vinyl-2,6-dimethoxyphenol. Molecular weight: 180.

Materials and methods

Materials and reagents. 4-Vinyl-2,6-dimethoxyphenol (canolol with a molecular mass of 180) was purchased from Junsei Chemical, Tokyo, Japan. It was synthesized to at least 95% purity (confirmed by nuclear magnetic resonance). The preparation was sealed under helium or nitrogen and maintained at -80˚C. Canolol was dissolved in ethanol and diluted in a serum-free medium immediately before the experiments. Gastric cancer SGC-7901 cells were obtained from the Department of Pathogeny Biology, Norman Bethune Medical College of Jilin University, China. Human gastric mucosal epithelial cell line GES-1 was obtained from the Cancer Hospital of Beijing University. The study protocol was approved by the ethics committee of the First Hospital of Jilin University.

Cell culture and treatment. Human SGC-7901 gastric cancer cell line and human GES-1 gastric mucosal epithelial cell line were cultured in RPMI-1640 medium containing 10% heat-inactivated fetal bovine serum (FBS) and 100 ng/ml each of penicillin and streptomycin in an incubator (50 ml/l CO_2) at 37˚C. The medium was changed every 2-3 days. Cells in the logarithmic growth phase were collected for subsequent experiments. The cells were treated with various concentrations of canolol for 24 h.

Cell viability assay. The method of 3-(4,5-dimethylthiazol-2-yl)-2,5-diphenyltetrazolium bromide (MTT) assay was employed to determine cell viability. Cultured SGC-7901 and GES-1 cells were detached using trypsinization, centrifuged at 1,000 x g for 5 min and resuspended in fresh RPMI-1640 medium. The cells were plated at a density of $5x10^3$ cells/well in 96-well microplates and treated with canolol ranging from 25 to 1,200 μmol/l for 24 h at 37˚C. At the end of treatment, 20 μl of MTT stock solution was added to each well [(0.5 mg/ml in phosphate-buffered saline (PBS)] for 4 h. The medium was replaced with 150 μl DMSO to dissolve the converted purple dye in the culture plates. Absorbance was measured at 570 nm on a spectrophotometer microplate reader. Cell viability was assayed as the relative formazan formation in treated compared with control wells after correction for background absorbance. Four wells per dose were counted in each experiment. Analyses were performed using SPSS version 10.0 (SPSS Inc, Chicago, IL, USA). Data were evaluated using one-way ANOVA. $P<0.05$ was considered statistically significant.

Cell morphology. SGC-7901 and GES-1 cells were seeded at a density of $5x10^5$ cells/well onto a cover slip loaded in 6-well plates. Fresh RPMI-1640 medium containing different concentrations of canolol was added. Cells were photographed with an inverted microscope under x200 magnifications to observe morphological changes.

Annexin V-FITC/PI staining for flow cytometry. SGC-7901 cells were collected and centrifuged at 1,000 x g for 5 min and resuspended in fresh RPMI-1640 medium at a density of $2x10^5$ cells/ml. Apoptotic and necrotic cells were evaluated by Annexin V (AV) binding and propidium iodide (PI) uptake using an AV-FITC-PI apoptosis assay kit (Pharmingen, San Diego, CA, USA). Samples were analyzed by flow cytometry.

Real-time quantitive PCR analysis. Total RNA of SGC-7901 cells was extracted using an RNA extraction kit and primers used are shown in Table I. Following DNase treatment, the first strand cDNA was synthesized. Quantitive PCR of Bcl-2, Bax and COX-2 were performed with the Bio-Rad (Hercules, CA, USA) CFX system. To exclude variations caused by RNA quantity and quality, the GAPDH gene was used as an internal control. Analyses were performed using SPSS version 10.0 (SPSS Inc). Data were evaluated using one-way ANOVA. $P<0.05$ was considered a statistically significant result.

Results

Canolol does not exhibit evident toxicity to GES-1 cells. The proliferation effect of canolol was determined using an MTT assay and GES-1 cells were used as a control to detect the cell toxicity of canolol. Cells were treated with different concentrations of canolol (0-1200 μmol/l). The data indicated that canolol has no obvious cytotoxicity against normal GES-1 cells. The percentage of cell viability was 99.38±3.57% at 25 μmol/l, 87.82±2.55% at 800 μmol/l and decreased to 65.31±4.44% at 1200 μmol/l (Fig. 2). Cell morphology using an inverted microscope also showed that cell structures were intact and were well established after 1,200 μmol/l canolol treatment (Fig. 3).

Canolol inhibits proliferation and induces apoptosis of SGC-7901 cells. SGC-7901 cells were treated with different concentrations of canolol (0-1200 μmol/l). The percentages of cell viability at various canolol doses were determined as the percentage of viable treated cells in comparison with

Table I. Primer sequences used in real-time quantitive PCR.

Gene	Primer sequence	Annealing temperature (°C)	Product size (bp)
COX-2	F: CTCCCTTGGGTGTCAAAGGTA R: GCCCTCGCTTATGATCTGTC	76	171
Bcl-2	F: GAGTTCGGTGGGGTCATG R: GGAGAAATCAAACAGAGGC	83	186
Bax	F: GGATGCGTCCACCAAGAA R: GAGCACTCCCGCCACAAA	83.5	388
GAPDH	F: AACGGATTTGGTCGTATTG R: GGAAGATGGTGATGGGATT	78.5	258

GAPDH, glyceraldehyde-3-phosphate dehydrogenase; F, forward; R, reverse.

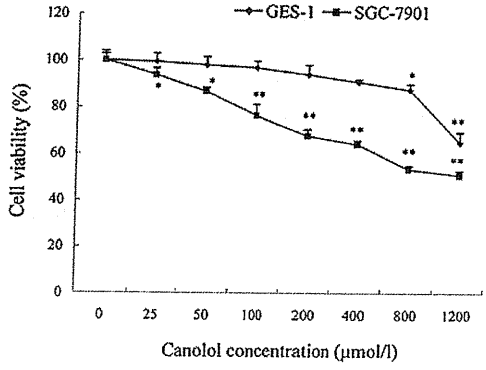

Figure 2. Effect of canolol on cell viability under different concentrations on particular cells using 3-(4,5-dimethylthiazol-2-yl)-2,5-diphenyltetrazolium bromide (MTT) assay (mean ± SD) (n = 4). Data were evaluated using one-way ANOVA. *P<0.05, **P<0.01.

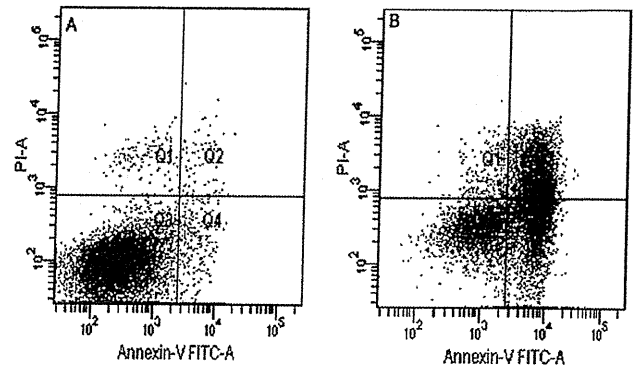

Figure 4. Apoptosis of SGC-7901 cells was investigated using a flow cytometry assay using FITC-Annexin-V/PI staining. (A) SGC-7901 cells without canolol; (B) SGC-7901 cells with 400 μmol/l canolol.

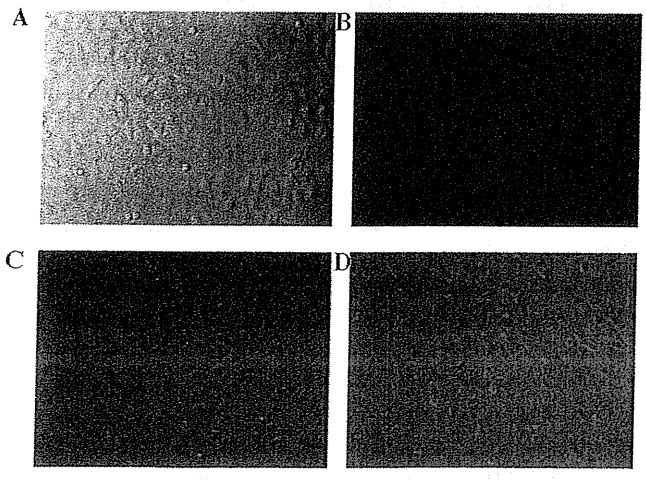

Figure 3. Morphology of GES-1 and SGC-7901 cells treated with 1,200 μmol l canolol.

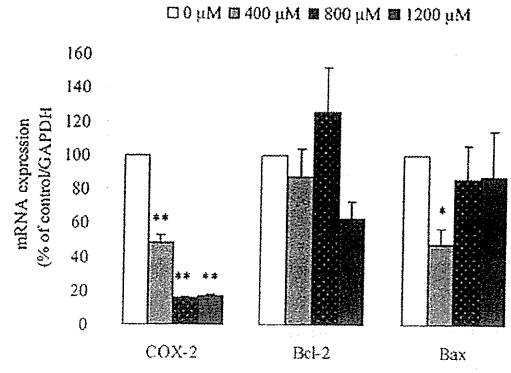

Figure 5. Relative expression levels of COX2, Bcl-2 and Bax mRNAs in SGC-7901 cells under treatment of different concentrations of canolol (mean ± SD) (n=3). Values are arbitrary unit values (mean ± SD) relative to 100 for controls. GAPDH was used as an internal control. Data were evaluated using one-way ANOVA. *P<0.05, **P<0.01 vs. control.

viable untreated cells. The results provided solid evidence that the inhibitory effects on the proliferation of canolol to SGC-7901 cells were dose-dependent (Fig. 2): the percentage of cell viability was 89.80±2.83% at 25 μmol l, 73.73±1.51% at 800 μmol l (P<0.05) and 51.22±1.82% at 1,200 μmol l (P<0.01). Consistent with the MTT assay results, the adherent SGC-7901 cells were markedly decreased and showed apoptosis under the treatment of 1,200 μmol l canolol (Fig. 3).

Furthermore, a flow cytometric analysis was used to quantify the rate of cell apoptosis using double staining of Annexin

V-FITC and PI. As shown in Fig. 4, the lower right field (high Annexin V, low PI staining) represents the early apoptotic cells due to the strong affinity of Annexin V-FITC with phosphatidylserine, which transports from the inner to the outer surface of the plasma membrane during early apoptosis. By contrast, the higher left field (high PI, low Annexin V staining) represents the necrotic cells, since PI, which binds to nucleic acids, only cross through the compromised membrane of dead cells or late apoptotic cells (17). Viable cells are shown in the lower left field (low Annexin V and PI staining) and the higher right field (high Annexin V and PI staining), indicating late apoptotic cells. The results showed that canolol was able to induce the apoptosis of SGC-7901 cells and the rate of early apoptosis, late apoptosis and necrosis of SGC-7901 cells were increased under 400 μmol/l canolol (Fig. 4).

Canolol downregulates the mRNA expression level of COX-2. To clarify the mechanisms of SGC-7901 cell apoptosis under canolol treatment, the mRNA expression level of COX-2, Bcl-2 and Bax was evaluated using real-time quantitive PCR. The sequences of these primers were shown in Table I. The results showed that in SGC-7901 cells, the relative mRNA expression level of COX-2 was decreased to 48.50±4.67% in 400 μmol/l, 16.08±0.75% in 800 μmol/l and 17.22±0.88% in 1,200 μmol/l canolol. The effect of canolol on COX-2 expression was downregulated ($P<0.01$); However, the expression levels of Bcl-2 and Bax fluctuated slightly (Fig. 5). These data suggested that the inhibition of COX-2 might play an important role in the apoptosis of SGC-7901 cells.

Discussion

Gastric cancer is one of the most prevalent malignant tumors and its morbidity is the highest in China. Currently, many natural and synthesized compounds are used in the chemoprovention and treatment of gastric cancer (18,19). Canolol, 4-vinyl-2,6-dimethoxyphenol, which is extracted from crude canola oil, has the ability to prevent *H. pylori*-infected gastric carcinogenesis in gerbils (10). In the present study, it was demonstrated that canolol prevented proliferation and induced apoptosis of SGC-7901 cells dose-dependently *in vitro*. Additionally, it had low toxicity to immortalized GES-1 cells (Figs. 2 and 3). The results indicated that canolol has the potential to be developed as a new natural anti-gastric carcinoma agent.

COX-2 is important in the conversion of arachidonic acid to prostaglandin H_2. Accumulating evidence suggests that the constitutive overexpresion of the inducible COX-2 gene is involved in a diverse array of cancers and Harris *et al* (20) demonstrated that COX-2 overexpresion initiated and promoted carcinogenesis through: i) mutagenesis, i.e., the production of certain reactive oxygen species that are carcinogenic; ii) mitogenesis, i.e., cell proliferation promoted by PGE-2 and other factors; iii) anti-apoptosis, i.e., cell differentiation and apoptosis reduced by PGE-2 and other factors; iv) angiogenesis, metastasis and immunosuppression (20). The real-time quantitive PCR in this study showed that COX-2 expression was downregulated under canolol treatment ($P<0.01$) (Fig. 5). It was postulated that inhibition of COX-2 expression may result in blockade of the prostaglandin cascade and a decrease in reactive oxygen species (ROS), thus stimulating apoptosis of malignant cells and preventing neoplastic growth. The scavenging potency of canolol against $ROO^{\cdot}$ is much higher than that of well-known antioxidants, such as α-tocopherol, vitamin C and β-carotene (21). A previous study in this laboratory showed canolol decreased serum 8-OHdG, a key biomarker of oxidative DNA damage relevant to carcinogenesis (10). Other natural phenolic extracts, such as BCE (black currant extract) and dioscin, reduce the risk of gastric cancer owing to their antioxidative functions (22-24).

Selective and non-selective COX-2 inhibitors may be involved in the intervention and chemoprevention of carcinogenesis (25-27). A series of epidemiologic studies found that the COX-2 inhibition levels of coxibs were consistent with their chemopreventive effects in cancers of the breast, colon, prostate and lung (20). Ma *et al* (28) have demonstrated that PGE2 acts with a family of G-protein-coupled receptors participating in multiple signal tranduction pathways.

The Bcl-2 family, such as Bax, Bad, Bid, Bcl-2 and Bcl-x, is one of the most extensively studied groups of proteins involved in cell apoptosis. Bax, Bad and Bid were shown to activate apoptosis, while Bcl-2 and Bcl-x were shown to inhibit the process (29). Transfection of COX-2 constitutive expression vector into the BCC cell line significantly upregulated Bcl-2 expression and this indicated that Bcl-2 might participate in COX-2 mediated anti-apoptic processes (30). In addition, the expression level of Bax, a member of a pro-apopotic protein family was downregulated in a transgenic mouse model (31). However, in the present study, no correlation between Bcl-2/Bax and COX-2 expression was found (Fig. 5).

The relationship between apoptosis and COX-2 downregulation in this gastric adenocarcinoma cells should be studied. COX-2 is a potential pharmacologic target that may be used in the prevention and treatment of various types of malignancies.

Acknowledgements

This study was supported by the National Natural Science Foundation of China (Nos. 30972476 and 81273065). The authors would like to thank Dr Yu Chen for technical support.

References

1. Ferlay J, Shin H R, Bray F, *et al*: Estimates of worldwide burden of cancer in 2008: GLOBOCAN 2008. Int J Cancer 127: 2893-2917, 2010.
2. Liu X, Zhang B, Guo Y, *et al*: Down-regulation of AP-4 inhibits proliferation, induces cell cycle arrest and promotes apoptosis in human gastric cancer cells. PLoS ONE 7: e37096, 2012.
3. Chuah SK, Tsay FW, Hsu PI and Wu DC: A new look at anti-*Helicobacter pylori* therapy. World J Gastroenterol 17: 3971-3975, 2011.
4. Graham D Y. Antibiotic resistance in *Helicobacter pylori*: implications for therapy. Gastroenterology 115: 1272-1277, 1998.
5. Siegel R, Naishadham D and Jemal A: Cancer statistics. CA Cancer J Clin 62: 10-29, 2012.
6. Kountouri AM, Kaliora AC, Koumbi L and Andrikopoulos NK: In-vitro gastric cancer prevention by a polyphenol-rich extract from olives through induction of apoptosis. Eur J Cancer Prev 18: 33-39, 2009.
7. Alvarez-Suarez JM, Dekanski D, Ristić S, *et al*: Strawberry polyphenols attenuate ethanol-induced gastric lesions in rats by activation of antioxidant enzymes and attenuation of MDA increase. PLoS One 6: e25878, 2011.

8. Jaganathan SK and Supriyanto E: Antiproliferative and molecular mechanism of eugenol-induced apoptosis in cancer cells. Molecules 17: 6290-6304, 2012.
9. Vaux DL and Korsmeyer SJ: Cell death in development. Cell 96: 245-254, 1999.
10. Cao XY, Tsukamoto T, Seki T, *et al*: 4-Vinyl-2,6-dimethoxyphenol (canolol) suppresses oxidative stress and gastric carcinogenesis in *Helicobacter pylori*-infected carcinogen-treated Mongolian gerbils. Int J Cancer 122: 1445-1454, 2008.
11. Harris RE, Chlebowski RT, Jackson RD, *et al*: Breast cancer and nonsteroidal anti-inflammatory drugs: prospective results from the Women's Health Initiative. Cancer Res 63: 6096-6101, 2003.
12. Kilic G, Gurates B, Garon J, *et al*: Expression of cyclooxygenase-2 in endometrial adenocarcinoma. Eur J Gynaecol Oncol 26: 271-274, 2005.
13. Targosz A, Brzozowski T, Pierzchalski P, Szczyrk U, Ptak-Belowska A, Konturek SJ and Pawlik W: *Helicobacter pylori* promotes apoptosis, activates cyclooxygenase (COX)-2 and inhibits heat shock protein HSP70 in gastric cancer epithelial cells. Inflamm Res 61: 955-966, 2012.
14. Ashok V, Dash C, Rohan TE, Sprafka JM and Terry PD: Selective cyclooxygenase-2 (COX-2) inhibitors and breast cancer risk. Breast 20: 66-70, 2011.
15. Ozalp SS, Eren CY, Bostancioğlum RB and Koparal AT: Induction of apoptosis and inhibition of cell proliferation by the cyclooxygenase enzyme blocker-nimesulide in the Ishikawa endometrial cancer cell line. Eur J Obstet Gyn Reprod Biol 164: 79-84, 2012.
16. Sun SY, Hail JRN and Lotan R: Apoptosis as a novel target for cancer chemoprevention. J Natl Cancer Inst 96: 662-672, 2004.
17. Tripathi M, Singh BK, Mishra C, Raisuddin S and Kakkar P: Involvement of mitochondria mediated pathways in hepatoprotection conferred by *Fumaria parviflora Lam*. Extract against nimesulide induced apoptosis in vitro. Toxicol In Vitro 24: 495-508, 2010.
18. Wu XY, Wang YL, Wang HW, *et al*: Quinacrine inhibits cell growth and induces apoptosis in human gastric cancer cell line SGC-7901. Cur Ther Res Clin Exp 73: 52-64, 2012.
19. Ji YB, Qu ZY and Zou X: Juglone-induced apoptosis in human gastric cancer SGC-7901 cells via the mitochondrial pathway. Exp Toxicol Pathol 63: 69-78 2011.
20. Harris RE, Beebe J and Alshafie GA: Reduction in cancer risk by selective and nonselective cyclooxygenase-2 (COX-2) inhibitors. J Exp Pharmacol 6: 491-496, 2012.
21. Dong X, Li ZR, Wang W, Zhang WJ, Liu SZ and Zhang XM: Protective effect of canolol from oxidative stress-induced cell damage in ARPE-19 cells via an ERK mediated antioxidative pathway. Mol Vis 17: 2040-2048, 2011.
22. Jia N, Xiong YLL, Kong BH, Liu Q and Xia XF: Radical scavenging activity of black currant (*Ribes nigrum L.*) extract and its inhibitory effect on gastric cancer cell proliferation via induction of apoptosis. J Funct Foods 4: 382-390, 2011.
23. Gao LL, Li FR, Jiao P, *et al*: Paris chinensis dioscin induces G2/M cell cycle arrest and apoptosis in human gastric cancer SGC-7901 cells. World J Gastroenterol 17: 4389-4395, 2011.
24. Hu MM, Xu LN, Yin LH, *et al*: Cytotoxicity of dioscin in human gastric carcinoma cells through death receptor and mitochondrial pathways. J Appl Toxicol doi: 10.1002/jat.2715, 2012.
25. Fu SL, Wu YL, Zhang YP, Qiao MM and Chen Y: Anti-cancer effects of COX-2 inhibitors and their correlation with angiogenesis and invasion in gastric cancer. World J Gastroenterol 10: 1971-1974, 2004.
26. Harris RE: Cyclooxygenase-2 (COX-2) blockade in the chemoprevention of cancers of the colon, breast, prostate, and lung. Inflammopharmacology 17: 55-67, 2009.
27. Chan AT, Ogino S and Fuchs CS: Aspirin use and survival after diagnosis of colorectal cancer. JAMA 302: 649-658, 2010.
28. Ma X, Kundu N, Rifat S, Walser T and Fulton AM: Prostaglandin E receptor EP4 antagonism inhibits breast cancer metastasis. Cancer Res 66: 2923-2927, 2006.
29. Tsujimoto Y and Shimizu S: Bcl-2 family: life-or-death switch. FEBS Lett 466: 6-10, 2000.
30. Tjiu JW, Liao YH, Lin SJ, *et al*: Cyclooxygenase-2 overexpression in human basal cell carcinoma cell line increases antiapoptosis, angiogenesis, and tumorigenesis. J Invest Dermatol 126: 1143-1151, 2006.
31. Liu CH, Chang SH, Narko K, *et al*: Overexpression of cyclooxygenase-2 is sufficient to induce tumorigenesis in transgenic mice. J Biol Chem 276: 18563-18569, 2001.